

INVESTIGATING THE VARIABILITY OF URBAN TREE PHENOLOGY USING
VOLUNTEER-HOSTED PHENOCAMS

By

Maya Lynn Hall

Submitted to the

Faculty of the College of Arts and Sciences

of American University

in Partial Fulfillment of

the Requirements for the Degree of

Master of Science

In

Environmental Science

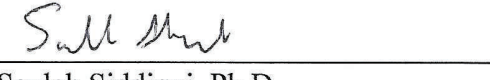
Chair:



Michael Alonzo, Ph.D.



Valentina Aquila, Ph.D.



Sauleh Siddiqui, Ph.D.



Dean of the College of Arts and Sciences

April 25, 2023

Date

2023

American University

Washington, D.C. 20016

© COPYRIGHT

by

Maya Lynn Hall

2023

ALL RIGHTS RESERVED

DEDICATION

To my mom, for always bringing me back to earth.

To my dad, for looking out for me from the stars.

INVESTIGATING THE VARIABILITY OF URBAN TREE PHENOLOGY USING
VOLUNTEER-HOSTED PHENOCAMS

BY

Maya Lynn Hall

ABSTRACT

The timing of vegetative phenology governs annual ecosystem function and is a component of community diversity and productivity. Consequently, phenology is key to monitoring and measuring ecological responses to environmental change. In cities, the timing of tree phenological events such as leaf unfolding and leaf coloring is altered due to regional climate factors like winter chilling length and spring warming temperatures, as well as site-specific variation such as land cover and genus. However, the variability of these changes to urban phenology, as well as the factors that govern variation, are not well explored. Likewise, while many studies use digital time-lapse cameras to study phenology in rural settings, few have used phenological cameras, phenocams, in the urban environment.

To investigate the phenology of urban trees using phenocams, this novel study used the city of Washington, D.C. to explore the interannual changes occurring in city trees, as well as the feasibility of using phenocams in combination with volunteer camera hosts. Phenocams were placed throughout the greater D.C. area in the homes of volunteers and on the campuses of two educational institutions. Each phenocam captured images of either a single tree crown or multiple over the course of three study years. From camera imagery, start of season (SOS) and end of season (EOS) were estimated by fitting a spline to each tree's green chromatic coordinate (Gcc) data, which were extracted at a near-continuous temporal resolution.

Statistical analysis revealed that there were significant differences in SOS between years. Further analysis of climatic and site variables found that temperature and impervious surface significantly influenced SOS and EOS respectively. Additional analysis showed that tree genera responded to annual changes in moderate synchrony. Assessment of community science implementation found that inclusion of volunteers increased the educational reach of the study, but likely created noise in the data due to issues such as accidental phenocam disturbance and repositioning. This novel study provides useful information for the methodology of future urban phenocam research and provides a preliminary understanding of phenology in the Washington, D.C. area.

ACKNOWLEDGMENTS

I wholeheartedly thank my advisor, Dr. Michael Alonzo, for supporting and guiding me through this research. I am grateful that he showed me the world of remote sensing and phenology, and I am even more grateful that he was always up for answering my (many!) questions. He helped me become a stronger, more confident scientist with his expertise, patience, and encouragement. I would also like to sincerely thank my committee members, Dr. Valentina Aquila and Dr. Sauleh Siddiqui, for their advice and expert knowledge. Their recommendations and support helped me bring this thesis to true fruition. I also want to thank Dr. Thu Ya Kyaw and Dr. Barbara Balestra. Dr. Kyaw generously helped me with my statistical methods and reminded me to breathe when said statistical methods did not make sense, and Dr. Balestra always had a kind and encouraging word to share with me throughout my time at American University. Lastly, I would like to thank my family and friends for always being sources of joy in my life.

TABLE OF CONTENTS

ABSTRACT.....	ii
ACKNOWLEDGMENTS	iv
LIST OF ABBREVIATIONS.....	x
CHAPTER 1: INTRODUCTION	1
CHAPTER 2: BACKGROUND	7
Phenology and Trees.....	7
Drivers of Phenology	9
Urban Phenology	11
Methods of Phenology Data Collection.....	13
<i>Field-Based Observations</i>	13
<i>Satellite Remote Sensing</i>	15
<i>Phenocams</i>	18
Community Science	22
CHAPTER 3: METHODS	24
Study Site	24
Phenocam Installation and Data Collection	26
Phenocam Image Processing.....	28
Statistical Analyses	33
<i>Testing Annual Differences in Phenometrics</i>	33
<i>Preparation of Climate Data</i>	33
<i>Preparation of Site Data</i>	34
<i>Preparation of Genus Data</i>	35
<i>Hierarchical Mixed Effects Modeling</i>	36
<i>Ordinary Least Squares Modeling</i>	38
Examination of Genera Differences.....	39
Assessment of Volunteer Participation.....	40
CHAPTER 4: RESULTS	41
Phenocam Performance	41
Phenological Differences Between Years.....	43
Hierarchical Mixed Effects Model Outputs.....	49
Ordinary Least Squares Model Outputs.....	52

Visualization of Genera Differences.....	56
Evaluation of Volunteer Inclusion	61
CHAPTER 5: DISCUSSION.....	63
Interannual Differences in Phenology	63
The Effect of Preceding Temperatures on Phenometrics	64
The Effect of Site Variables on Phenology.....	66
Genera-Level Differences in Phenometrics	67
Phenocams and Community Science	69
CHAPTER 6: CONCLUSION	73
REFERENCES	75

LIST OF TABLES

Table 1. Codes assigned to the genera within this study.....	30
Table 2. Candidate predictor variables with descriptions.	36
Table 3. Data collection status for each phenocam. Active status indicates that the phenocam was actively gathering data, while inactive means that the phenocam was no longer collecting data.	42
Table 4. Results of the Tukey's HSD test run for SOS.....	44
Table 5. Selected climate variable values representing six-month SOS temperature averages (C°), six-month EOS temperature averages (C°), and six-month precipitation sums for EOS (in.)	50
Table 6. Hierarchical mixed effects model performance indicators.	51
Table 7. SOS hierarchical mixed model summary.....	51
Table 8. EOS hierarchical mixed model summary.	52
Table 9. Ordinary Least Squares model performance indicators.	53
Table 10. SOS OLS model.....	54
Table 11. EOS OLS model.....	55
Table 12. Monthly mean temperatures (C°) for January, February, March, and April of the study period.....	68

LIST OF ILLUSTRATIONS

Figure 1. 30-meter resolution satellite imagery in RGB of the Washington, D.C. area from Landsat. Each pixel within the image represents 30x30 meters. The inset map provides visual differences between canopy or vegetation-dominant land cover (green center portion of the map) and land dominated by impervious surfaces (mixed colors to the left and right of the inset)	17
Figure 2. Example of phenocam imagery from HoS South phenocam.	19
Figure 3. Washington, D.C. study site with district borders outlined in orange and each phenocam location is symbolized as a bright blue circle.....	25
Figure 4. Example of near-ideal set up at Delaware Ave. phenocam site. FOV contains more canopy than sky and there is minimal glare within the frame.	26
Figure 5. Examples of phenocam set-ups. Top: Outdoor phenocam mount on roof. Bottom Left: Protective case and screen view. Bottom Right: Indoor phenocam suction mount on window.....	27
Figure 6. Example of drawn ROIs on phenocam imagery. Crown ROIs are drawn in blue for each tree within the study. Each tree is assigned a label that corresponds to the species, as well as a unique identifying number. Invariant targets (non-crown objects that persist in the FOV) are also identified and labeled.	29
Figure 7. Examples of multi-year spline interpolations for three phenocams and three different Chinese Elm (<i>Ulmus parvifolia</i>) individuals. Each gray point represents a Gcc value per DOY. The blue points represent spline fit. The gray horizontal dashed line is the baseline established for each tree. Spaces between the spline fit indicate absence of data (typically from periods during winter and summer). The green plus signs designate SOS and the red plus signs represent EOS. A) Tree 1007 from the 17 th St. phenocam. B) Tree 1009 from the First St. phenocam. C) Tree 1004 from the Trinidad Ave. phenocam.....	33
Figure 8. SOS variability by year.	45
Figure 9. Annual early spring (January – April) temperature averages.....	46
Figure 10. EOS variability by year.	47
Figure 11. Precipitation sums for the six months preceding EOS for each year.	48
Figure 12. GSL variability by year.	49
Figure 13. Fractional impervious surface cover by mean EOS. The blue line represents the line of fit and the green area of the plot represents the confidence interval. Data points are colored by phenocam location.	56
Figure 14. Boxplots of SOS by genus.....	57

Figure 15. Boxplots of EOS by genus.....	58
Figure 16. Median SOS plotted against year and colored by genus. Gaps in genera data are produced by missing phenocam data due to phenocam withdrawal, FOV complications, or data loss from technical malfunctions.....	59
Figure 17. Median EOS plotted against year and colored by genus.....	60
Figure 18. Monthly temperature averages for each study year. The historic average of each month is labeled as "Norm" and colored in bright red.....	65
Figure 19. Median phenometric values for each genera plotted across three years. A) SOS, B) EOS (Alonzo et al. accepted).....	68

LIST OF ABBREVIATIONS

ANOVA	Analysis of Variance
BIC	Bayesian Information Criterion
DOY	Day of Year
ELEV	Elevation Variable
EOS	End of Season
EVI	Enhanced Vegetation Index
FOV	Field of View
Gcc	Green Chromatic Coordinate
GSL	Growing Season Length
HSD	Honest Significant Difference
IMP	Impervious Surface Variable
MAD	Median absolute deviation
NDVI	Normalized Difference Vegetation Index
OLS	Ordinary Least Squares
PRECIP	Precipitation Variable
Q-Q	Quantile-Quantile
RGB	Red-Green-Blue
RMSE	Root-mean-square-error
SD	Secure Digital
SOS	Start of Season
TCF	Fractional Tree Canopy Variable
TEMP	Temperature Variable
UFD	Urban Forestry Division
UHI	Urban Heat Island
varImp	Variable Importance
VIF	Variance Inflation Factor

CHAPTER 1

INTRODUCTION

Phenology refers to the seasonal, recurring events in the lives of plants and animals. The phenology of trees is influenced by climate conditions such as temperature and precipitation, as well as local or site-specific factors such as impervious surfaces, elevation, and fractional canopy cover (Cleland et al. 2007, Wang et al. 2014). Understanding and monitoring tree phenology, hereafter referred to as simply phenology, is crucial to understanding ecological patterns in the natural world, as well as predicting ecosystem responses to small and large environmental changes (Cleland et al. 2007). In particular, phenology plays a significant role in how other ecological and biological processes function under shifting environmental conditions. Changes in phenology such as earlier spring budburst or longer periods of vegetative growth can affect species diversity, alter carbon and water cycling, and affect the resilience of an ecosystem (Richardson et al. 2018, Teets et al. 2023).

Much of the phenology research done today uses satellite imagery to monitor rural or natural areas (Richardson et al. 2007). Satellites enable the collection of repeat data over large regions of the earth and are an effective tool for tracking phenology over time. Unfortunately, satellites are often overly coarse in their temporal and spatial resolutions, which makes them suitable for large-scale studies focused on broad trends, but less appropriate for investigating fine scale phenological details (Richardson et al. 2007). In addition, the technique of using satellite imagery to monitor phenology is not optimally accessible to the public and does not often naturally allow for the implementation of community science. To fill the knowledge and utility gaps in satellite imagery, digital repeat photography has become a useful method to capture phenology at the canopy level.

Phenological cameras, phenocams, are time-lapse cameras that can be mounted nearly anywhere and used to continuously obtain phenology data. By remaining at canopy or near-surface level, phenocams generate important information about local and species-specific phenology without the concern of low temporal or spatial resolution (Richardson et al. 2007, Richardson et al. 2018). Like satellites, phenocams have been increasingly used in research that focuses on natural areas such as research plots, protected parks, or other vegetation-heavy landscapes. However, favoring rural areas as study sites limits understanding of both local and global phenology as urban sites are highly influential to both broad environmental conditions and phenological responses.

Urban landscapes are rapidly growing and have an increasing impact on the environment (Zhang et al. 2004, Alonzo et al. 2021, Zhang et al. 2022). Cities are characterized by heterogenous land cover distribution, and impervious surfaces such as roads and sidewalks affect the heating and cooling of urban areas, which ultimately elevates city temperatures relative to the surrounding land (Alchapar et al. 2014, Melaas et al. 2016). Consistent elevated temperatures in cities produce anomalous phenological responses in trees such as earlier leaf unfolding and flowering (Zipper et al. 2016). These anomalies have been thoroughly studied in the context of regional or global phenology, as well as through field observations and satellite remote sensing techniques. However, there is a dearth of studies that incorporate phenocams as the primary method of data collection from urban areas. **To address the relative lack of phenocam studies in cities and to better understand local phenological change, this research project explored the methodology of installing volunteer-hosted phenocams in the city of Washington, D.C. and examined the influence of climate and site variables on urban phenology.**

This exploratory study uses 2020-2022 red-green-blue (RGB) imagery of canopies from 19 phenocams with unique locations to investigate (1) the impacts that seasonal climate conditions have on phenology, (2) the influence that site-specific variables have on D.C. phenology, and (3) the methodology of using phenocams hosted by volunteer community scientists. Based on these guiding topics, three research aims were developed:

Aim 1: Test the extent to which phenocam imagery can track urban phenology changes influenced by regional air temperature and precipitation.

Phenological change is driven by a multitude of external and internal factors (e.g., temperature, species, etc.; Jochner and Menzel 2015, Richardson et al. 2018). In temperate forests, temperature is particularly influential (Vitasse et al. 2009, Basler and Körner 2014, Geng et al. 2020). Recent decades of warming have advanced a number of phenological events including spring bud development, leaf unfolding, and flowering (Chmielewski and Rötzer 2001, Melaas et al. 2013, Xie et al. 2015, Jochner and Menzel 2015). In addition, higher temperatures have extended the length of the growing season, which pushes some autumn phenological responses to later in the year (Luo et al. 2006, Richardson et al. 2010). Precipitation also plays a key role in temperate phenology as certain precipitation patterns, for example summer droughts or wet springs, may initiate phenological shifts in tree populations (Jin et al. 2019, Vitasse et al. 2021).

In cities, trees are subject to elevated temperatures as a result of the Urban Heat Island (UHI) effect, which may further alter phenological events (Zhang et al. 2004, Luo et al. 2007, Imhoff et al. 2010). Due to the nature of their composition, urban areas are also composed of higher percentages of impervious surface cover, which have an impact on the heating and

cooling of the area, as well as the movement and storage of water after a precipitation event (Alchapar et al. 2014, Melaas et al. 2016, Song et al. 2016, Zipper et al. 2016). As the climate changes and cities experience elevated temperatures, it is necessary to better understand how phenology, measured by phenological metrics (phenometrics) such as start-of-season (SOS), end-of-season (EOS), and growing-season-length (GSL), changes, as well as the mechanisms behind notable shifts. In rural areas, the synchronicity of phenological events like SOS and seed dispersal has been shown to be influenced by temperature and microclimatic variability, and is a significant driver of the behavior and success of other species (Koenig et al. 2015, Geng et al. 2020, Dai et al. 2021). It is likely that D.C.'s urban trees are responding similarly to climatic changes, but whether phenocams can adequately capture urban phenological shifts and interannual variation induced by climate is still unknown.

This research uses phenometrics gathered from phenocam imagery, along with minimums, maximums, and averages of daily and monthly temperature data, as well as mean monthly precipitation data, to examine the effect of climate conditions on D.C.'s phenology. It is expected that phenocams will be able to detect urban phenological responses to changing climate conditions between and within years. In particular, it is anticipated that phenocams will capture an advance of SOS and a delay of EOS under the conditions of elevated temperature, as well as a delay in both SOS and EOS under the conditions of reduced precipitation.

Aim 2: Explore the variability of urban tree phenological responses across phenocam site and genera.

Within a city, trees typically maintain the same physiological tolerances or limitations as their rural counterparts; however, the addition of urban-related site factors like impervious

surfaces and reduced canopy cover can influence phenological changes (Luo et al. 2007, Melaas et al. 2016, Alonso et al. 2021). Such changes are normally attributed to global temperature increases or UHI, but greater examination of the impact of site variables can reveal the strength of governance that location has on phenology. In addition, phenology, and sensitivity to shifts in climate conditions, can vary by species or genera due to differences in physiology (Schaber and Badeck 2003, Basler and Körner 2014, Kalusova et al. 2017, Fréjaville et al. 2019). These differences can account for the success of genera in certain geographic areas, as well as provide explanations for absent or failed populations in particular habitats. Investigation of the genera-level differences in urban phenometrics can provide helpful insight into observed variation.

In order to better understand the effect that site and genus have on urban phenology, this study models site variables (impervious surface cover, fractional canopy cover, and elevation) to determine which factors have a significant effect on phenometrics. Likewise, differences in phenometrics across the genera of this study are analyzed and visualized to reveal how genus may affect the timing of phenological events in urban areas.

The observed phenological responses within this study are expected to react strongly to D.C. site variables. Specifically, high percentages of impervious surface cover and low fractional canopy cover will produce advanced SOS and delayed EOS. Changes to phenological responses have also been attributed to physiological differences, so it is also expected that reasonable variation among the tree genera of this study will exist; however, the rank order of trees is anticipated to stay the same from year to year.

Aim 3: Examine the suitability of phenocams as reliable and practical tools for urban phenology studies and explore the implementation of volunteers as phenocam hosts.

Existing research has shown that phenocams are a useful tool for gathering phenological data. Not only do phenocams provide large quantities of data, but they also do not have the constraint of coarse spatial and temporal resolutions that occur with satellite imagery. Many studies incorporate phenocams in an effort to capture phenological change across rural landscapes. Less common, however, is the use of phenocams within urban areas. Given that the methodology of this study is novel, the evaluation of method success will be mainly descriptive in nature. To assess the suitability of phenocams for the urban landscape, the procedure used has been recorded, and additional information has been gathered from volunteer interactions. Volunteer feedback will also be used to describe the successes and challenges from this study. Important factors include phenocam reliability and data fidelity across multiple study years. Instances of field of view (FOV) change or image interference will be included to provide an understanding of the complexity of installing and maintaining phenocams over multiple years in a city.

CHAPTER 2

BACKGROUND

Phenology and Trees

Phenology is the timing of natural recurring life cycle events. Examples of phenology in trees include leaf unfolding and flowering in the spring, leaf coloring in autumn, and dormancy during winter (Jochner and Menzel 2015). These phenological events, which are sometimes referred to as phenophases, signal the switch between vegetative state to reproductive state (flowering to seed set). Phenological events vary among species and are important for maintaining community diversity and ecosystem productivity (Cleland et al. 2007). In addition, phenology is a regulator of ecosystem processes and biosphere feedbacks to the climate system and serves as a monitor for global climate change (Zhou et al. 2016, Richardson et al. 2018).

Due to the influence that trees have on other species, understanding their phenology and potential shifts in phenological responses is necessary to managing, maintaining, and protecting ecosystems and communities. Trees provide a multitude of services for a vast number of species, including humans, and create valuable habitat and nursery spaces (Solomon 1997, Kirschbaum 2003, Nowak et al. 2007, Chaparro and Terradas 2009, Stagoll et al. 2012, Peters et al. 2016). It is estimated that some tree species host and support hundreds to thousands of animal species, and consequently contribute to both floral and faunal biodiversity (Southwood et al. 2005, Prevedello et al. 2017, Threlfall et al. 2017). Similarly, in both tropical and temperate forests, needle or leaf fall, as well as tree falls, return rich nutrients to the soil and act as catalysts for new life (Meier et al. 2005).

Importantly, tree phenology serves as an indicator or initiator for other species' phenological responses (Polgar et al. 2013, Vitasse et al. 2021). For instance, leaves changing colors in the autumn may supplementally signal to migratory bird species that it is time to begin migrating (McGrath et al. 2009, Mayor et al. 2017). Correspondingly, many species rely on the products of tree phenological events to support their various life stages (Southwood et al. 2005). Springtime flowering and the development of fruits and nuts provide critical food sources for pollinators, frugivores, and granivores, while buds and leaves offer herbivores nourishment throughout the growing season (Peters et al. 2016). The influx of nutrition subsequently prepares species for the reproductive season and contributes to the continuance of populations.

Just as trees are essential to the functioning of other living organisms, so too are they crucial to abiotic processes and cycles within ecosystems. Trees act as soil stabilizers, water and air filters, and shade promoters. Tree roots hold soil in place, which increases overall soil stability, as well as slows the flow of water to prevent soil loss due to erosion (Daynes et al. 2013, Ford et al. 2016, Williams et al. 2018, Miri and Davidson-Arnott 2021). Trees filter water by promoting the ground absorption of rainfall and taking up water through their roots. In addition, they filter the air by absorbing carbon dioxide and trapping airborne particulate matter on their leaves (Vailshery et al. 2013, Shukla and Srivastava 2019, Letter and Jäger 2020). Lastly, trees cool local air temperatures by creating valuable shade and through the release of water via transpiration (Tscharntke et al. 2011, Li and Ratti 2018, Sabrin et al. 2020).

Given the vital role that trees play for both individual species and entire ecosystems, it is necessary to understand how they are behaving and possibly changing from year to year. Studying and monitoring phenology provides in-depth knowledge about the cumulative productivity of an ecosystem and can uncover seasonal abnormalities. For example, growing

season length (GSL) in deciduous forests is derived from the number of days that plants are actively growing, and acts as a control on many tree services. Shifts in GSL can quantitatively describe productivity changes (i.e., shifts to tree growth and contribution of energy and biomass to a system) and help predict how ecosystems will respond to shifting environmental conditions in both the near and distant future.

Drivers of Phenology

Globally, climate is extremely influential to phenology, with factors such as annual precipitation and average temperature playing important roles in the phenological responses of trees (Chmielewski and Rötzer 2001, Ferreira and Parolin 2007, Günter et al. 2008). The phenology of trees and forests in different regions of the world will often correspond to different climatological drivers. In tropical forests, phenology will typically respond to annual precipitation levels, as well as changes in irradiance (Chapman et al. 2018, Wright and Calderón 2018). Thus, the timing of flower to fruit is more heavily dependent on the rainy season than it is on large fluctuations in temperature (Cleland et al. 2007, Davis et al. 2022). By contrast, temperate forests are more frequently governed by photoperiod and air temperature, which historically align with the seasons, to induce specific phenological responses such as turning red in the fall or breaking dormancy in the spring (Menzel 2003, Basler and Körner 2014, Kabano et al. 2021).

Alterations in temperature (e.g., lack of a cold enough winter chilling period, hotter spring, etc.) affect the phenological response of plants and subsequently change the natural processes and functions of other species (Vitasse et al. 2009, Zipper et al. 2016). Examples of these types of changes have already been observed; earlier spring onset and budbursts lead to

phenological mismatches in other species, while later autumn senescence has implications for the following year's SOS (Menzel and Fabian 1999, Walther et al. 2002, Jochner and Menzel 2015, Liu et al. 2016, Richardson et al. 2018, Geng et al. 2020).

Shifts in phenological response highlight the potential for greater ecosystem disruptions that could be more difficult to predict and manage. As such, differences in phenological response, both local and regional, have become instrumental to understanding global environmental change. Similarly, as temperatures increase and weather patterns fluctuate due to anthropogenic climate change, phenology becomes an increasingly important measure of ecosystem response (Richardson et al. 2010, Richardson et al. 2018).

Another external driver of phenology is the site or geographic location of a tree (Jochner et al. 2012, Pellerin et al. 2012, Dai et al. 2021, Zhang et al. 2022). Site-specific conditions, such as the topography (i.e., slope and elevation) of an area, as well as the soil composition and amount of surrounding impervious surfaces, can alter or influence changes in phenology. For instance, trees that are at higher elevations are typically going to have different or delayed phenology compared to trees that live at sea level (Pellerin et al. 2012). Similarly, the immediate landscape surrounding a tree may influence or shift phenological events (Vitasse et al. 2021). Higher percentages of impervious surface cover have been associated with higher air temperatures, which lead to advanced SOS, variable GSL, and delayed EOS (Mimet et al. 2009, Jochner et al. 2012, Zhang et al. 2022). Likewise, lower fractional tree canopy cover has been shown to decrease the effectiveness of temperature mitigation by trees, which reduces a tree's ability to resist deleterious phenological change (Greene and Kendron 2018).

While climatic conditions and site act as significant drivers of phenology, genus or species-specific attributes can also influence the timing of phenophases and lead to distinct

differences in the aggregate phenological response of different areas (Chuine et al. 2000, Valdez-Hernández et al. 2010, Wright and Calderón 2018, Geng et al. 2020, Vitasse et al. 2021, Kabano et al. 2021). Condition tolerances (e.g., sensitivity to temperature) and physiology (e.g., wood density, xylem water potential, etc.) both inform species distribution and productivity, which in turn influence phenology (Morin et al. 2009, Valdez-Hernández et al. 2010). Similarly, age or maturity can affect an individual's phenology and produce varied phenological reactions to environmental changes (Vitasse et al. 2009, Basler and Körner 2014, Fréjaville et al. 2019). Observing genus and species differences in phenological response is important for monitoring the complex communities that rely on trees and forests and for predicting and mitigating species' responses to climate change.

Changes to interspecies differences in phenology may instigate greater ecosystem shifts, which are more difficult to swiftly adjust or adapt to for plant and animal communities (Vitasse et al. 2009, Basler and Körner 2014). For example, due to its physiology and growth pattern, an aspen species (*Populus tremuloides*) may naturally break dormancy earlier than an oak species (*Quercus alba*). This order of breaking dormancy is synchronous with the needs and behavior of aspen and oak-reliant animals. However, under the influence of increased mean global temperatures the aspen may delay breaking its dormancy, which alters the pattern and order of trees' phenological events. Ultimately, changes such as this have strong impacts on the ecological and biological processes of other species and entire ecosystems (Morin et al. 2009).

Urban Phenology

Phenological change is occurring throughout many different regions and ecosystems of the world and requires continued monitoring and examination (Cleland et al. 2007). In urban

ecosystems, phenology is traditionally less well-investigated (Jochner and Menzel 2015, Melaas et al. 2016). This is in part due to the complex relationship between nature and the structure of urban areas. In cities, the ecological and biological functions of the environment can be dramatically different from the surrounding natural land. Urban areas, which are characterized by high human density and strong material and landscape heterogeneity, are home to approximately 55% of the world's population, with an expected increase to 68% by the year 2050 (World Bank 2020). These unique ecosystems function under human management and often incorporate synthetic materials and structures such as buildings and roads with natural elements in the form of parks or gardens. Despite the inclusion of some natural components, urban areas are overwhelmingly dominated by impermeable surfaces and artificial materials that vary in heat capacity and conductivity (Landsberg 1981, Jochner and Menzel 2015).

The thermophysical properties (albedo, emissivity, rugosity, etc.) of the materials used in a city greatly influence the area's overall temperature and potentially alter the function and timing of ecosystem services within that urban ecosystem (Landsberg 1981, Alchapar et al. 2014). More specifically, buildings, roads, and other surfaces increase the absorption of shortwave radiation, decrease energy loss by emission of longwave radiation, and have reduced evapotranspiration. The sum influence of these properties contributes to heat generation, retention, and reduced cooling ability (Melaas et al. 2016). In addition, urban areas tend to inherently have far fewer trees and patches of vegetation-heavy green space. The lack of trees and other vegetation reduces an area's ability to cool air temperatures via transpiration and decreases shaded zones (Sabrin et al. 2020). Combined, the loss of both air temperature cooling and shade patches emphasizes the distinct difference between urban and rural temperatures.

Urban areas have been found to be as much as 2.9 °C warmer than surrounding non-urban areas (Imhoff et al. 2010). This significant difference leads to a phenomenon known as the Urban Heat Island (UHI) effect. UHI is characterized by increased temperatures in urban zones relative to the temperatures of the surrounding rural land and has a serious impact on plant phenology (Zipper et al. 2016, Melaas et al. 2016). UHI can contribute to an advance of SOS, extension of EOS, and subsequently lengthen a tree's GSL. These alterations to phenology have equally significant impacts on water, energy, carbon, and climate. Even small changes to the phenology of an urban landscape may introduce local environmental and ecological issues such as reduced ecosystem services, as well as compound shifts in GSL that are already occurring due to climate change (Menzel and Fabian 1999, Schwartz and Reiter 2000, Zipper et al. 2016).

Due to the addition of the UHI effect, trees in cities are experiencing warming faster, and perhaps more intensely, than trees or forests in rural landscapes, and may serve as a proxy and predictor for environmental responses to future global environmental and climatological change (Jochner and Menzel 2015). Monitoring how trees and their phenology respond to the elevated temperatures and unique conditions in cities provides key insight and acts as an important tool to investigate what may be expected for all ecosystems and areas under the influence of a changing climate in the coming years.

Methods of Phenology Data Collection

Field-Based Observations

Historically, phenological observations were made using on-the-ground visual assessments by individuals or groups (Richardson et al. 2018). Certain phenological events such

as the first development of buds or leaf-out are often conveniently visible, and studies using field techniques have provided a plethora of phenological information, as well as advanced the study of phenology (Badeck et al. 2004, Luo et al. 2007, Wallace et al. 2016). Today, visual, or hands-on assessments from the field are still used to obtain phenological information, which contributes to a wide variety of disciplines and informs both scientific and environmental policy efforts (Browning et al. 2017). These methods allow for the collection of tree-specific data, as well as the incorporation of volunteers, students, and other scientists in diverse fields of study (Theobald et al. 2015). However, on-the-ground and sight-based phenological data often require a significant amount of time and energy. To collect enough data for statistical analysis, there is often the need for frequent repeated trips to field study sites, which may be difficult to access depending on the area of focus. Additionally, there often is the need to recruit, hire, and train more than one person to obtain the data within a reasonable fieldwork timeframe and this may incur higher project costs or increase the likelihood of data-gathering errors (Liang and Fei 2012, Rosemartin and Miller-Rushing 2021).

Another challenge of field observations is the difficulty in capturing change over large areas through time. Often, teams working on a project can only cover a select area, which provides intensive data about that specific site, but misses broader details due to limited spatial coverage (Studer et al. 2007). To address this deficiency, remote sensing arose in the mid to late 1900s as a new method of gathering phenological data. Remote sensing is a form of data collection that relies on satellites or aircrafts to obtain large data sets that contain landscape-level information. Satellites have proven particularly useful in the capture of comprehensive land cover and phenological data (Townshend et al. 2012, White et al. 2002, Melaas et al. 2013, Jin et al. 2019).

Satellite Remote Sensing

Satellites orbit the earth and receive or relay a variety of information depending on their intended purpose (Dunbar 2015). Starting in the 1970s, satellite remote sensing was used to obtain land cover data and track landscape-level or global trends and changes (Reed et al. 1994). Satellites record the spectral reflections of light emitted from each type of land cover and produce imagery that can follow phenological change over large areas.

Satellites collect information at varying temporal frequencies and spatial resolutions. The frequency of data collection and the resolution depend entirely on the satellite and are useful to a variety of research methods and topics (Reed et al. 1994, Studer et al. 2007). Some satellites, such as Landsat, collect repeat data of the earth's surface every 16 days. Others, like Sentinel 2, collect repeat data approximately every 10 days, while Moderate Resolution Imaging Spectroradiometer (MODIS) collect data daily (The European Space Agency (ESA), n.d., The National Aeronautics and Space Administration (NASA), n.d.). Products specific to phenological studies, such as the land surface phenology (LSP) product derived from Harmonized Landsat Sentinel-2 (HLS) data, can provide datasets that track phenophase transitions at 30m spatial resolution and a temporal frequency of three days (Bolton et al. 2020).

From collected spectral reflections, information about the landscape can be extracted and analyzed using a variety of vegetation indices. These indices quantitatively and qualitatively evaluate vegetative land cover using the wavelengths returned to the satellite from each cover type (Bannari et al. 1995). Commonly used indices, such as the Normalized Difference Vegetation Index (NDVI) and Enhanced Vegetation Index (EVI), rely on red and near-infrared (NIR) reflectances or radiances (Fang et al. 2014). Since vegetation absorbs visible light (specifically red and blue wavelengths) and strongly reflects near-infrared wavelengths, indices

like NDVI enhance the contrast between vegetation and non-vegetation (e.g., bare soil or rooftop; Los et al. 2000).

Distinguishing between land cover types provides comprehensive characterization of phenological observations across complex landscapes. Many studies have used satellite imagery's ability to generate such large quantities of repeat data with wide spatial coverage to detect large-scale shifts in phenology. For example, satellite imagery has revealed that much of the northern hemisphere is experiencing an earlier onset of spring and a delay in the start of fall phenological events, which correspond to ground-based observations about phenological shifts (Studer et al. 2007, Jin et al. 2019).

Due to the wide spatial coverage and opportunity for repeated temporal sampling, satellites are a popular method for monitoring global phenology (Zhang et al. 2003). Despite their popularity, there are a few limitations to monitoring and extracting phenological data using satellites. Namely, there are limits to satellites' temporal and spatial resolutions. Satellites in orbit can only revisit an image location once a day or after a few days or weeks depending on the satellite. This means that satellites are lower in temporal resolution and may be missing minute changes throughout a landscape (Townshend and Justice 1988, Townshend et al. 2012). It is also important to note that if cloud cover, smoke, or other interferences occur, then the observations cannot be repeated until the satellite revisits the location, so valuable data are at risk of being lost.

Satellites are also constrained by their spatial resolution. An image from a satellite will provide a spatial resolution of anywhere from 10m to 1000m. Images captured from Landsat, for example, will have a spatial resolution of 30m, which means that at minimum each pixel in the image will represent a 30x30 meter area (Figure 1). This is still a fairly large area when

considering the information required to identify species and differentiate between individuals and site variability (Moon et al. 2021).

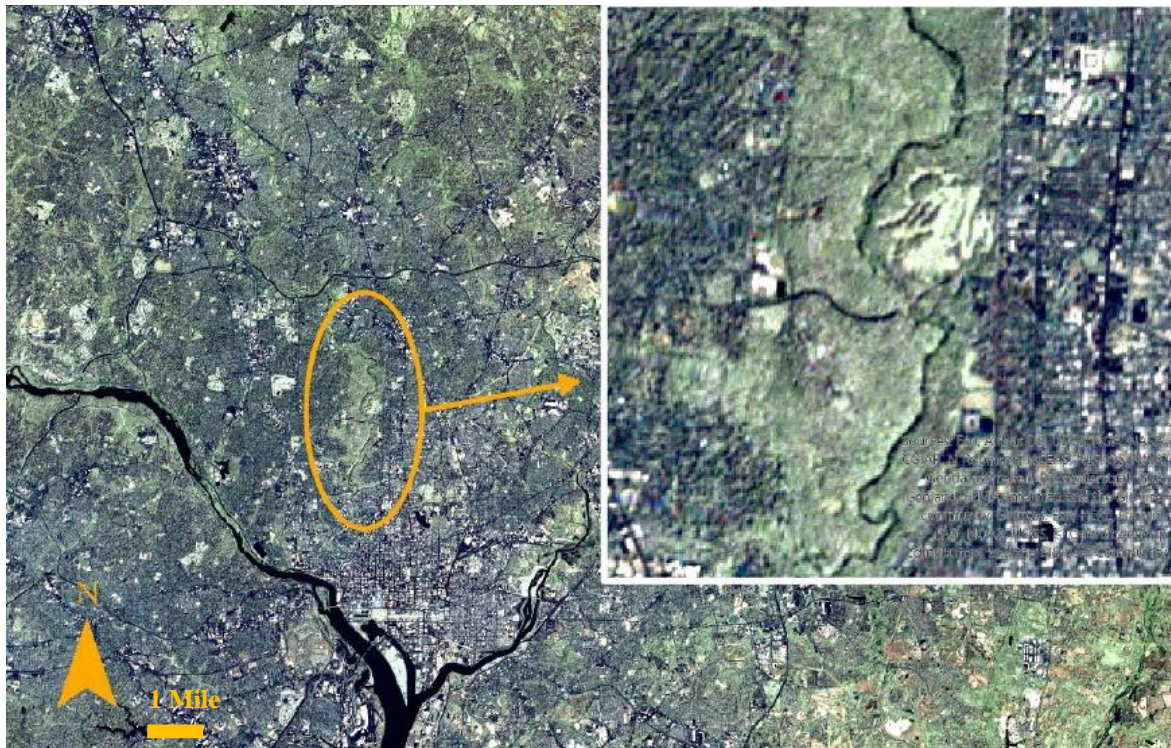


Figure 1. 30-meter resolution satellite imagery in RGB of the Washington, D.C. area from Landsat. Each pixel within the image represents 30x30 meters. The inset map provides visual differences between canopy or vegetation-dominant land cover (green center portion of the map) and land dominated by impervious surfaces (mixed colors to the left and right of the inset).

Research that uses satellite imagery also needs to account for image quality complications. There can be frequent image contamination by clouds or other atmospheric interferences like smoke from a fire (Richardson et al. 2007). Image contamination can influence data, prevent any phenological data from being usable, and may interrupt or delay research for extended periods of time. Additional disturbances or limitations include improper calibration of equipment or satellite orbit drifts (Los et al. 2000, Studer et al. 2007). Due to the potential

constraints on satellite imagery in phenology studies, another technique that uses near-surface repeat digital photography has risen in use within recent decades.

Phenocams

Phenocams are digital time-lapse cameras that remain stationary and capture nearly continuous images of a canopy (Richardson et al. 2007). Typically, phenocams are mounted high on flux towers, which are meteorological towers that measure multiple atmospheric and environmental parameters such as gas exchanges and energy. Once stationed on a tower, phenocams are aimed at the canopy with the intention of maximizing the percentage of canopy seen within the field of view (FOV) (Richardson et al. 2018). The imagery from phenocams is much finer in spatial resolution than satellites and has a reduced likelihood of atmospheric interference due to phenocams' near-surface locations. Phenocams vary in style and price, which optimizes flexibility, but may occasionally cause differences in image analysis due to variation in camera settings (sensor type, light sensitivity, etc.) (Sonnenstag et al. 2012).

Most studies using phenocams focus on natural areas since phenocams are typically set up within active forests or research plots (The PhenoCam Network, n.d.). By nature of their near-surface setup, phenocams can be used to investigate individual tree crowns or whole canopies (Richardson et al. 2018). Likewise, phenocams can be used to determine species differences or similarities, which is difficult to do using satellite imagery (Figure 2).

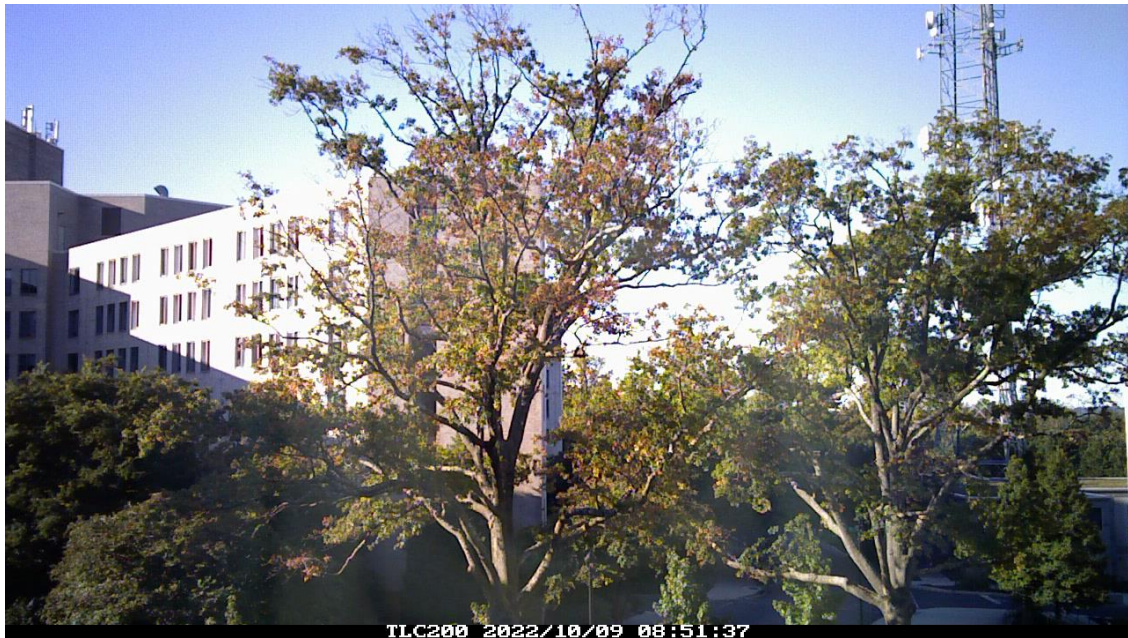


Figure 2. Example of phenocam imagery from HoS South phenocam.

To provide useful phenometrics, phenocams capture canopy or crown images in red, green, and blue wavelengths (RGB). Occasionally, phenocams will also capture images in near-infrared, but many phenocam studies rely on the visible light spectrum of red-green-blue (RGB) (Graham et al. 2010, Richardson et al. 2018, Aasen et al. 2020). Standard protocols for setting up and using phenocams were developed by the PhenoCam Network (Richardson et al. 2018). To reduce lens flare and shadowing, phenocams should ideally be pointed north in the northern hemisphere and south in the southern hemisphere. The FOV for each phenocam should contain more than 50% canopy and less than 50% sky, with an ideal mix of 80% canopy and 20% sky. Additionally, the PhenoCam Network recommends mounting phenocams in protective cases at a height of 5-10m above the canopy to obtain a level horizon and stable FOV. Mounting the cameras above the canopy reduces the risk for phenocam disturbance and decreases camera movement. These protocols encouraged high quality data from phenocams and standardized the participating digital time-lapse cameras within the network.

Many phenocam studies similarly follow a structured protocol for gathering and processing phenocam data. Phenocams can be set to capture images at varying times throughout a single day, with some studies utilizing time intervals as small as fifteen minutes (Richardson et al. 2007). During image analysis, a region of interest (ROI) is identified, for example a single crown that exists throughout the timeseries, and the pixels within the ROI are examined to produce ROI-specific RGB information (Richardson et al. 2018, Seyednasrollah et al. 2019).

Within the ROI, the combination of RGB wavelengths in each pixel can be separated into distinct channels or layers, which allows for the distinction and comparison of the red layer to the green layer, the blue to the green layer, and so on. To achieve RGB values for the entire ROI, RGB pixel values are averaged to produce a digital number representing single RGB values. From the RGB information, the intensity, or brightness, of each individual color can be calculated (Seyednasrollah et al. 2019). Using the intensity of each color, the “greenness” of trees in the ROI can be produced by using vegetation or color indices.

Two indices that are useful in phenocam data analysis are excess green (ExG) and green chromatic coordinate (Gcc) (Gillespie et al. 1987, Sonnentag et al. 2012, Aasen et al. 2020). Both ExG and Gcc can be used to determine differences between green plants and non-green targets (e.g., soil or bare branches), but Gcc has been shown to be more effective than ExG at suppressing any interfering daily or seasonal effects (Sonnentag et al. 2012). Gcc is calculated using the following formula:

$$Gcc = \frac{G}{R + G + B}$$

The formula for Gcc normalizes the green in an image against the red and blue colors. By quantitatively measuring the “greenness” of the canopy, it is possible to differentiate between

canopy conditions throughout each data collection period (Reid et al. 2016). Thus, Gcc can be tracked over various time increments, such as months or years, or phenophases (spring, summer, etc.) and can be compared to the inverse function of red chromatic coordinate (Rcc) to display tree green-up in the spring through leaf-fall in the autumn. The measurement of “greenness” is used as a tracking metric for phenology and can help explain when trees are the greenest during a time period, which trees are turning green faster or slower, and how greenness (representing phenology) shifts over time.

Thanks to their relative ease of use, phenocams and their accompanying indices are used throughout many different ecosystems to track phenological change. In the tropics, phenocams have aided in detecting unique characteristics of tree phenology that are instigated by flowering and leaf coloring (Nagai et al. 2016). In arid environments, phenocams have been shown to provide better interpretations of land surface phenology (Browning et al. 2017). Similarly, in grasslands and temperate forests phenocams are proven to be suitable tools for monitoring phenology of both herbaceous and woody plants (Sonnentag 2012, Inoue et al. 2015, Richardson et al. 2018).

Although there has been an increase in both phenology studies and research using phenocams in recent years, urban areas have not received much attention. Time-lapse cameras in the urban environment are nearly ubiquitous and phenology of urban ecosystems is instrumental in understanding both local and global shifts, but the complex structure and spatial layout of cities may have previously discouraged the wide use of phenocams. Despite the unique conditions of urban areas, it is important to explore using phenocams as the primary method of phenological data collection since they may offer a flexible, accessible, and reliable solution to monitoring urban phenology at the canopy level.

Community Science

Citizen science, which is also known as community science, engages members of the public in scientific projects, in-depth research, and surveys (Dickinson et al. 2010, Vogt and Fischer 2014, Theobald et al. 2015, McKinley et al. 2017, Roman et al. 2017). Community science has been incorporated into scientific research for decades and has allowed for progress across many different disciplines. In the ecological sciences, volunteers are typically recruited and trained when large quantities of data need to be collected and recorded, or when a study requires frequent, repeated observations (McKinley et al. 2017). Individuals or groups can participate in and get familiar with a scientific project as much as they desire and, depending on the project or topic, a variety of ages and skill-levels may get involved. The outcomes of utilizing community science are varied, but traditionally include increased environmental knowledge and awareness, improved scientific literacy, introduction to or enhancement of existing understandings of how to conduct a research project, and acquisition of new skills (Roman et al. 2017, McKinley et al. 2017).

Across many scientific fields, the engagement of volunteers and implementation of community science is not new. In earth observation and remote sensing studies, community participation has aided in the calibration and validation of imagery (Fritz et al. 2017). Similarly, forest and land cover research projects have benefited from the volunteer work of community members using both traditional data collection techniques (e.g., measuring stems with calipers) and newer methods (e.g., applications that measure diameter-at-breast-height (DBH) from an image taken on a mobile device like a cell phone) (Molinier et al. 2016). In phenology studies, community volunteers have helped to fill gaps in broad spatio-temporal datasets, as well as expanded the scope and scale of certain data gathering techniques (Kosmala et al. 2016). Notable

projects include Project Budburst, which asks community members to track climate change by collecting plant data, and Nature's Notebook, which relies on community members to collect phenological observations of plants and animals in an effort to inform environmental decision-making (Chicago Botanic Gardens 2021, USA National Phenology Network n.d.)

While all studies have found varying degrees of accuracy among volunteers, most agree that data gathered by trained volunteers are reasonably valid and differ only slightly from data gathered by professionals (Bloniarz and Ryan 1996, Roman et al. 2017). Frequently, the addition of community science complements existing data collection methods and is a useful tool to consider when collecting data. Overall, the outreach, education, and environmental motivation benefits of incorporating community science into scientific studies are often well worth the inclusion of volunteers when appropriate.

CHAPTER 3

METHODS

Study Site

The city of Washington, D.C. was used as the central location for this study. The geographic range of this research project extends from just north of the city (Silver Spring, Maryland) to the southern point of the city-proper (southwest quadrant). The greater D.C. area spans just over 68 mi² and is situated at an elevation of 125 meters mean sea level (MSL). The region is classified as a humid subtropical climate and is home to over 689,000 residents (United States Census Bureau 2020).

As of 2015, Washington, D.C. has approximately 38% tree cover that is distributed in patches and individual plantings (Alonzo et al. 2021). The general composition of native versus non-native species throughout the city approximates 73% native to North America and 27% non-native with origins in other countries. The area contains a large national park, Rock Creek Park, whose forests are dominated by American beech (*Fagus grandifolia*), boxelder (*Acer negundo*), and tulip tree (*Liriodendron tulipifera*), all of which are native to North America (Casey Trees 2015). The city's street trees are diverse with maples (*Acer*), oaks (*Quercus*), and elms (*Ulmus*) making up the majority of the trees in managed landscapes.

The dominant types of land cover not associated with the national park or canopy cover include grass at 22.8% coverage and tar at 20.7% coverage (Casey Trees 2015). An important aspect of land cover to note is the percentage of impervious surface cover. Within the immediate D.C. area, approximately 39% of land is covered by impervious surfaces (Alonzo et al. 2021).

These surfaces, which are defined by the inability of water to penetrate through them, influence the movement of stormwater, as well as heat and energy fluxes.

The location for each phenocam site was chosen from a pool of volunteer participants.

The volunteers were sourced from a local restoration-focused non-profit called Casey Trees.

Volunteers that had clear views of crowns or canopy were chosen as phenocam hosts. 16 phenocams were installed in individual volunteer homes, while two were installed on the campus of American University and one was installed at a local elementary school (Figure 3).

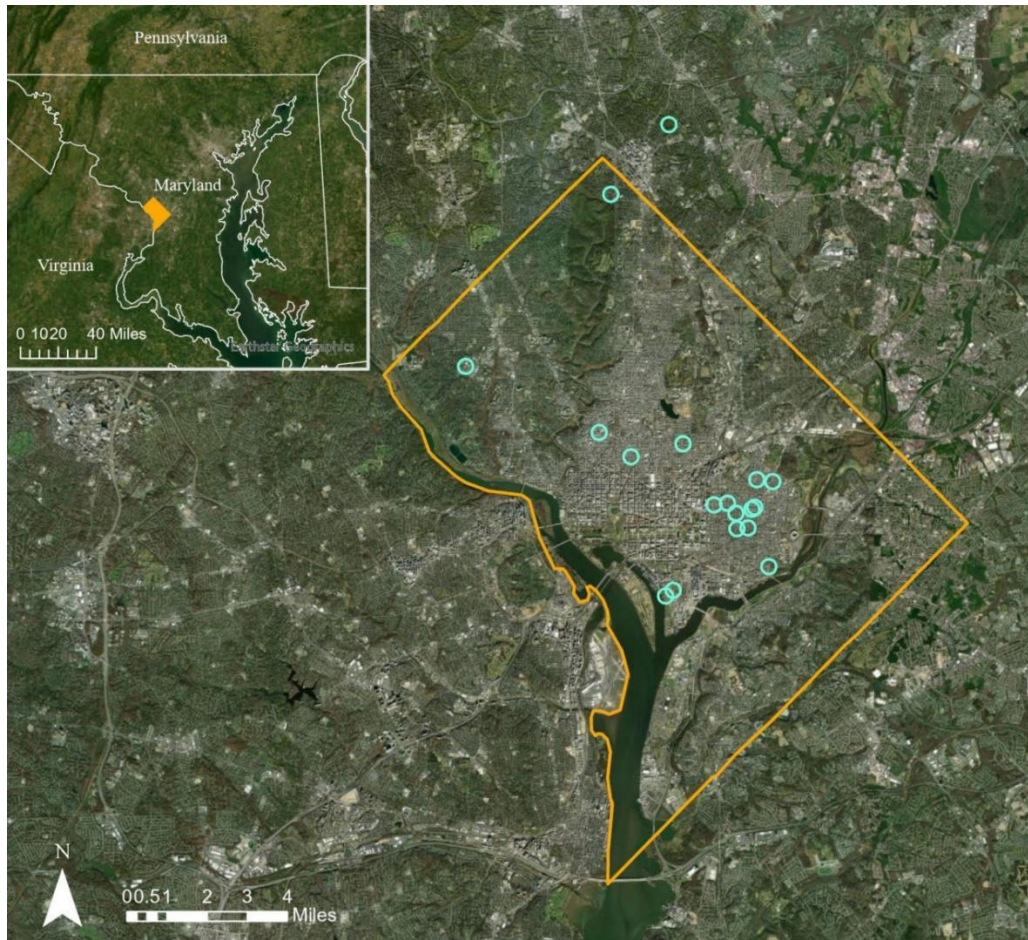


Figure 3. Washington, D.C. study site with district borders outlined in orange and each phenocam location is symbolized as a bright blue circle.

Phenocam Installation and Data Collection

The methodology for installing the phenocams was adapted from the standards developed by the PhenoCam Network. Phenocam set-up was altered to be site-specific in order to accommodate for the nature of the study and the site variation (e.g., roof or window view, direction, angle, etc.). North-facing views were preferred, as were sites that allowed the phenocam FOV to be filled with greater than 50% canopy (Figure 4).



Figure 4. Example of near-ideal set up at Delaware Ave. phenocam site. FOV contains more canopy than sky and there is minimal glare within the frame.

Phenocams were secured to roof mounts or suctioned to indoor windows. Outdoor phenocams were equipped with protective casings to prevent damage from rain, wind, and other conditions (Figure 5).



Figure 5. Examples of phenocam set-ups. Top: Outdoor phenocam mount on roof. Bottom Left: Protective case and screen view. Bottom Right: Indoor phenocam suction mount on window.

To produce data that captured near-continuous canopy conditions, each phenocam was set to take one picture every hour for each 24-hour period. All phenocams used four AA batteries and required a battery change roughly every 100 days. During these battery changes, the data were downloaded from the phenocam's Secure Digital (SD) card for image processing and analysis. Data were collected starting in 2019 through 2020; however, consistent data collection did not begin until 2020, so 2019 lacked sufficient data. Therefore, only the years 2020 to 2022 were considered in this study.

Phenocam Image Processing

All image processing and data analysis was performed in R. Raw data consisted of video files with each video representing one data collection period such as SOS 2021. Before analysis, the videos were separated into time-stamped hourly images. Following, the data were run through R script that selected the best daily image from each day. During best image selection, the brightness of each pixel was used to create an adaptive brightness threshold, which then located the best image per day. The collection of daily images was then manually reviewed for incorrect day and time labels, as well as poor image quality (e.g., images obscured by clouds or fog were replaced with higher quality images from the same 24-hour period).

Once the set of daily images for a phenocam was finalized, the images were input into an R package called xROI (Seyednasrollah et al. 2019). The xROI package launches a graphical user interface (GUI) that allows a user to draw regions of interest throughout a time series. For each phenocam, unique ROIs were drawn around target crowns and invariant targets. In most cases, each ROI represented an individual tree that was identified by the Urban Forestry Division (UFD) of Washington, D.C. (Figure 6).

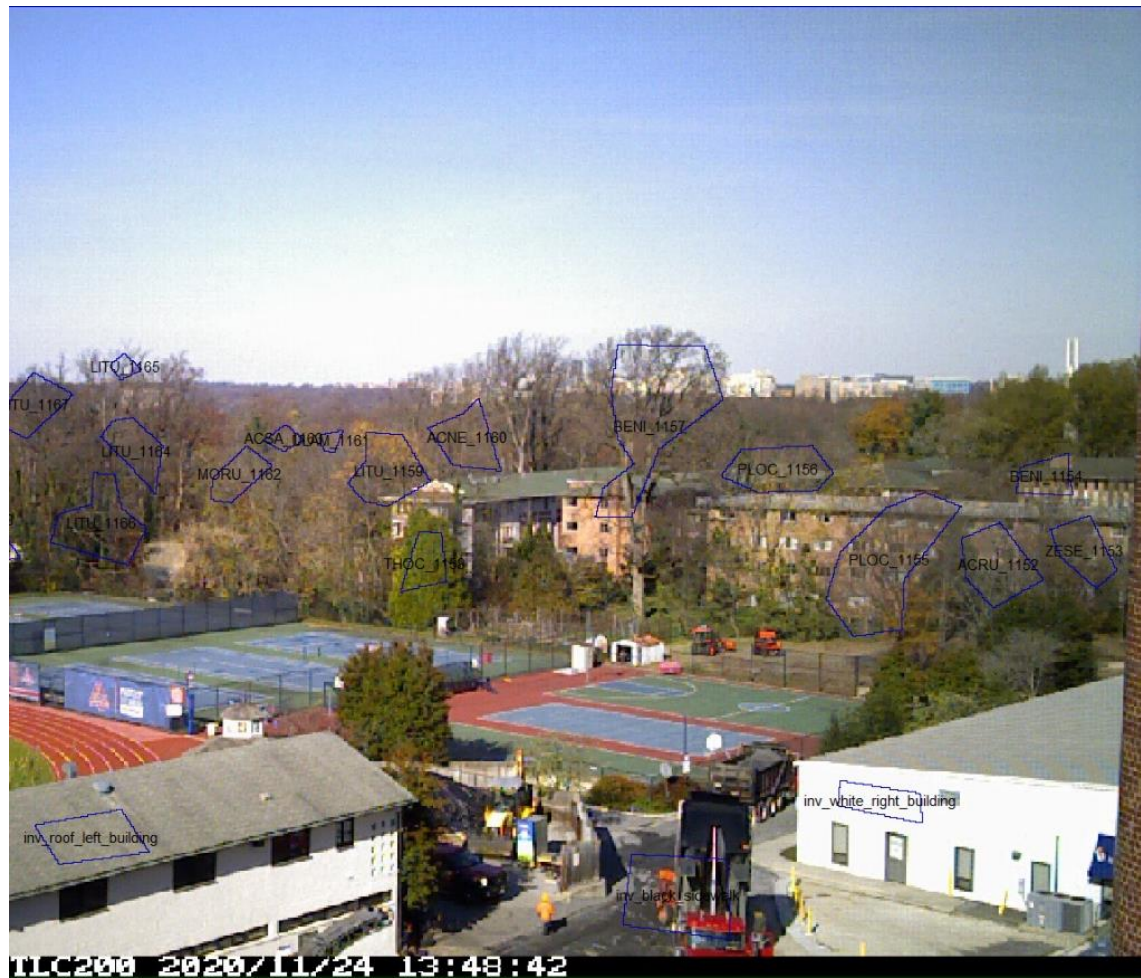


Figure 6. Example of drawn ROIs on phenocam imagery. Crown ROIs are drawn in blue for each tree within the study. Each tree is assigned a label that corresponds to the species, as well as a unique identifying number. Invariant targets (non-crown objects that persist in the FOV) are also identified and labeled.

Each identified tree crown was given a unique four-letter code, which corresponded to the species and genus of the individual (Table 1).

Table 1. Codes assigned to the genera within this study.

Code	Genus
ACSA	<i>Acer</i>
BENI	<i>Betula</i>
CABE	<i>Carpinus</i>
CECA	<i>Cercis</i>
CEO	<i>Celtis</i>
LAIN	<i>Lagerstroemia</i>
LIRO	<i>Liquidambar</i>
LITU	<i>Liriodendron</i>
MORU	<i>Morus</i>
NYSY	<i>Nyssa</i>
PLAC	<i>Platanus</i>
QULY	<i>Quercus</i>
ROPS	<i>Robinia</i>
ULAM	<i>Ulmus</i>
ZESE	<i>Zelkova</i>

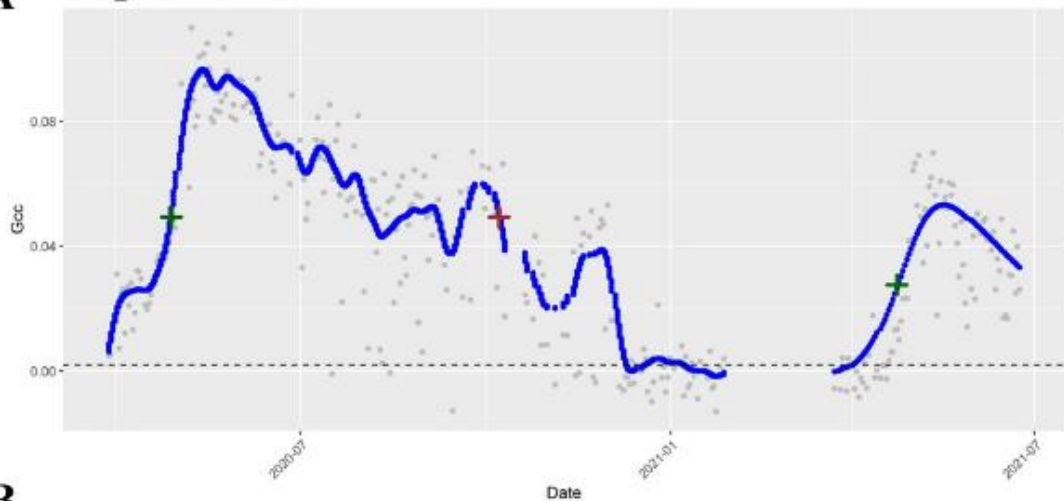
In instances where the canopy could not be divided into easily identifiable crowns, larger ROIs were drawn and named as “NI”, which indicated that the crowns were not identified to the genus or species level. Similarly, if trees did not have a UFD identification, then they were labeled as “NI”. Trees that were identified as conifers were given the label “NL”, or needleleaf. The unidentified individuals were included in broad phenometric analysis but removed during

analysis of phenometrics across genera. Needleleaf individuals were removed from all analyses due to their year-round persistence of green foliage.

The invariant targets included objects in the FOV that were not canopy and had a consistent presence throughout the study period, such as a rooftop or sidewalk. The invariant targets were included for the purpose of normalizing scene illumination across images. Once ROIs were drawn, all of the ROIs of a phenocam were saved as both a Tag Image File Format (TIFF) file and the adjoining vector information in the form of a comma separated values file (CSV). An intermediate code extracted color information and statistical metrics for each RGB chromatic coordinate, and calculated Gcc. Lastly, the metrics were prepped and saved as CSV files to be used in the final step of the data processing.

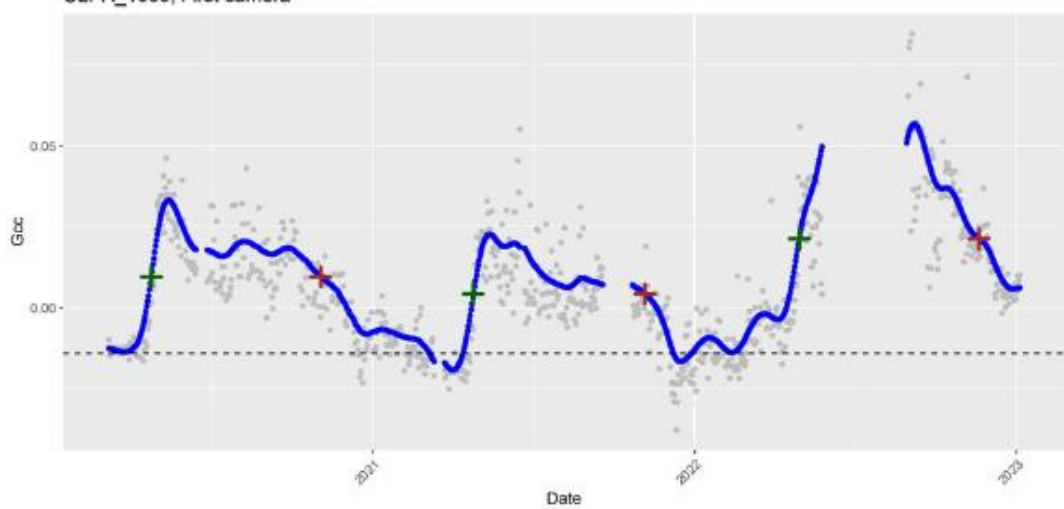
A multi-year spline fitting method was developed to both fit the data to a spline and generate phenometrics for each tree. For each phenocam moving window statistics were used to run a 75th percentile window over the data (Sonnenstag et al. 2012). Following, spline interpolation fit a cubic smoothing spline to Gcc data and added a baseline. SOS and EOS of each year were calculated from the mean of maximum Gcc values and the baseline, and then identified on the spline. GSL was manually calculated by subtracting SOS from EOS. The final outputs included a CSV file containing phenometrics, and the spline image which displayed the average Gcc value per day, the spline fit, and the day-of-the-year (DOY) when each phenometric occurred (Figure 7).

A ULPA_1007, 17th camera



B

ULPA_1009, First camera



C

ULPA_1004, Trinidad camera

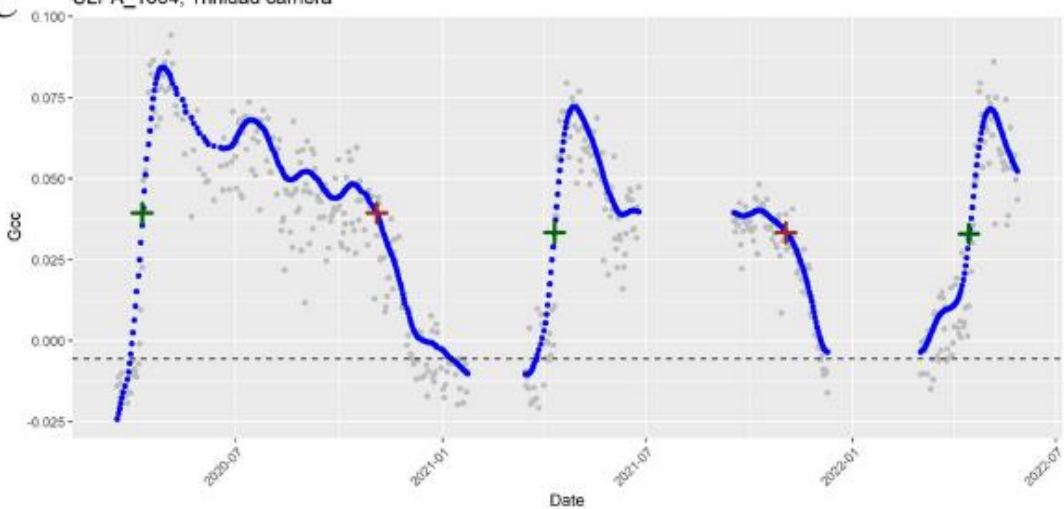


Figure 7. Examples of multi-year spline interpolations for three phenocams and three different Chinese Elm (*Ulmus parvifolia*) individuals. Each gray point represents a Gcc value per DOY. The blue points represent spline fit. The gray horizontal dashed line is the baseline established for each tree. Spaces between the spline fit indicate absence of data (typically from periods during winter and summer). The green plus signs designate SOS and the red plus signs represent EOS. A) Tree 1007 from the 17th St. phenocam. B) Tree 1009 from the First St. phenocam. C) Tree 1004 from the Trinidad Ave. phenocam.

Statistical Analyses

Testing Annual Differences in Phenometrics

To preliminarily determine whether phenocam imagery detected annual differences in phenometrics, the phenometric data were grouped by year. The grouped data were first checked for the assumption of normality using the Shapiro-Wilk test. Following, an analysis of variance (ANOVA) was run to determine whether significant differences existed between years for SOS, EOS, and GSL. Once significance was determined, Tukey's Honest Significant Difference (HSD) was used to identify which years were significantly different from one another. As a final step, boxplots were created to visualize and better interpret differences in phenometrics.

Preparation of Climate Data

To examine phenocam imagery in conjunction with interannual climate differences and to address Aim 1 of this study, regional climate data (air temperature and precipitation) were retrieved in monthly and daily means, maximums, and minimums from the National Oceanic and Atmospheric Administration (NOAA). To convert the climate data into a set of useful predictor variables, the air temperature and precipitation data were assembled into distinct variables that represented phenologically influential periods of time. In particular, variables were created based

on the understanding that preceding conditions in the winter affect spring phenological events, while preceding conditions in the summer affect autumn phenological events (Menzel 2003, Luo et al. 2006, Mimet et al. 2009, Pellerin et al. 2012, Basler and Körner et al. 2014, Wang et al. 2014, Liu et al. 2015, Xie et al. 2015, Jin et al. 2019, Alonzo et al. 2023). To produce the climate time periods for this study, the mean DOY of each phenometric was used to determine months and days that should be included in the preceding conditions. For example, the mean SOS value for 2020 was DOY 110 (April 19th), so all climate variables for 2020 were calculated with April 19th as the end date. The resulting variables included preceding three-month, six-month, and daily (10, 15, and 20 day) minimum, maximum, and average values for both air temperature and precipitation.

Preparation of Site Data

In order to investigate the objectives of Aim 2, phenocam site data were retrieved from a number of sources. Tree canopy cover and elevation data were obtained from a 2018 lidar Canopy Height Model (CHM) and 2018 lidar Digital Terrain Model (DTM) respectively. Impervious surface cover was derived from city planimetric data (Table 2). Additional temperature data for EOS were acquired from a 2018 study that collected a mobile air temperature value in D.C. on August 28, 2018 (Shandas et al. 2019). This single date variable was incorporated as a spatially varying predictor to capture localized air temperature anomalies that may influence the timing of EOS. This variable was applied to only EOS because the air temperature value was collected during a summer month. No mobile air temperature data were collected during an SOS-appropriate time.

The site data were incorporated into this study to provide a high-resolution assessment of drivers of urban phenology. Additionally, the site variables enabled quantitative characterization of the differences between each phenocam (e.g., local imperviousness). To process the site data, a shapefile of coordinates for every phenocam was overlaid on raster data of impervious surface cover, canopy cover, elevation, and the local air temperature. Each phenocam location was buffered by 5, 15, and 90 meters to establish the spatial magnitude of each variable. The inclusion of three different buffer sizes allowed for the comparison of varying neighborhoods of influence on each tree. The site data were then extracted from within each buffer. Once extracted, the fractional coverage of each variable was used in modeling (Table 2).

Preparation of Genus Data

Species information was also incorporated into this study to investigate the phenocams' ability to capture fine-scale differences between tree types and explore the synchronicity of urban trees from year to year. Species identities were acquired from the D.C. Department of Transportation's Urban Forestry Division (UFD) for street trees within the study. Trees that were not identified in the UFD data were named as "NI" during ROI processing. Any existing needleleaf trees were labeled as "NL" but were ultimately excluded in statistical analysis. Notably, although there were over 25 species included in this study, the number of each species varied highly, and thus species were grouped within their genus so that the genera could be implemented as a variable (Table 2).

Table 2. Candidate predictor variables with descriptions.

Variable Name	Short Name	Description
Tree canopy	TCF	1 m tree canopy map derived from 2018 City of D.C. lidar data
Impervious surface	IMP	Impervious surface from City of D.C. planimetric data
Elevation	ELEV	City of D.C. lidar Digital Terrain Model (2018)
Local Air Temperature	TEMP_18	Single-day local air temperature from Shandas et al. 2019
Regional Air Temperature	TEMP	Monthly and daily minimums, maximums, and averages from NOAA
Precipitation	PRECIP	Monthly averages and totals from NOAA
Genus	GEN	UFD-identified genera of trees from phenocam imagery

Hierarchical Mixed Effects Modeling

Statistical modeling was conducted to investigate the relationship between each variable and phenology. Exploring the relationship between interannual urban phenometrics and regional and local drivers is key to better understanding how influential each variable is to the phenological responses of trees. Additionally, meaningful inferences regarding the efficacy of phenocams can be drawn from characterizing these predictor variables and their effects on phenology.

During model testing, all relevant variables were standardized so that differences in the units of each variable could be removed. Standardization of the variables also aided in the interpretation of variable importance for each model. For all modeling, SOS and EOS were filtered to remove outliers. SOS was filtered to only include $SOS \leq DOY 180$, and EOS was filtered to include $EOS \geq DOY 270$. Given that SOS in this study is intended to represent spring phenological events, the DOY filter for SOS was chosen to remove any SOS values that were later than July. Similarly, the DOY filter for EOS was chosen to remove any values earlier than September since EOS in this study is only representing autumn phenological events.

A hierarchical mixed effects model was used to examine climate and site influences on SOS and EOS. The mixed modeling method was first applied to examine phenometrics nested within phenocam location. In addition, mixed modeling allowed for differentiation between the effects of the spatially distinct sites and the effects of differences in physiology (*genus*) and *year*, as well as variation in phenocam functionality and set-up.

The hierarchical mixed model regression was performed with the “lmer” function (from the *lme4* package), which allowed for the comparison of fixed and random effects in the model. The fixed effects were designated as the site variables, and the random effects were assigned to *genus*, *year*, and phenocam. Combinations of fixed effects and random effects were then tested to determine which variables had a significant influence on the phenometrics.

Multiple models were fitted to each phenometric response variable (SOS and EOS). During model assessment, variables were included or excluded through a number of steps. Existing literature informed general variable inclusion in this study, and initial variable testing examined variable combinations using *varImp* (variable importance), which provided the level of importance that each variable held in a given model. Subsequent testing included using Root-

mean-square error (RMSE) and median absolute deviation (MAD) values to track which variables improved model performance and which variables reduced model fit. RMSE assessed the difference between predicted and observed values in the models. Evaluation using MAD was included due to MAD's insensitivity to outliers and the presence of potentially noisy data. In addition, R-squared (R^2) values and coefficients were referenced to determine the explanatory power of each model. Minimization of the Bayesian Information Criterion (BIC) was used to select a single final model for each phenometric. Lastly, the model residuals and fitted values were plotted to reveal variances, and multicollinearity between variables was checked using Variance Inflation Factor (VIF).

Ordinary Least Squares Modeling

Following the hierarchical mixed effects modeling, Ordinary Least Squares (OLS) regression was used to examine the variable relationships without the influence of random effects. By not including random effects, the model is not overly influenced by broad grouping factors like *phenocam* or *year*. These random effects include sources of variance that are more difficult to quantify within this study. For example, *phenocam* effects may include variance due to shifts in FOV, phenocam angle and height, and disruptions to continuous data collection such as SD card malfunction. The variance produced by these sources is not generalizable and therefore is less useful to understanding the relationship between predictor variables and phenometrics.

OLS regression removed the random effects from the modeling process and minimized the total squared error, which enabled the comparison of multiple independent variables for both SOS and EOS. Similar to the mixed modeling procedure, varImp was used to preliminarily

assess variable importance, and RMSE was applied to determine each model's error. MAD was additionally included to account for potential outlier influences and provide a more robust indicator of model performance. R^2 values were compared to aid in determining model performance, and BIC minimization was used for selecting the final OLS models. Finally, residual and fitted values were plotted and potential heteroscedasticity was checked using the Breusch-Pagan Test for Homoscedasticity.

Examination of Genera Differences

In addition to modeling site and climate variables, the relationship between phenometrics and genus was investigated. Importantly, BIC excluded *genus* from all regression analysis, but preliminary examination of the *genus* variable across phenometrics and years provided useful information regarding general interspecific differences between the genera of this study.

To determine whether phenometrics differed significantly among genera, one-way ANOVAs were conducted. Following, the genera were filtered to remove any “NI” or “NL” individuals. This ensured that the phenometrics would only represent known trees. Phenometric differences were then visualized as boxplots to show the variability across genera.

As a final step, median phenometric values of each genus were compared across the three study years. The median of each phenometric was chosen for comparison given that the median values represent the typical phenometrics of each genus. Study year and median phenometric values were plotted and colored by *genus*. The resulting plots provided visual guidance and insight into the synchronicity of genera throughout the years, as well as the maintenance of rank order.

Assessment of Volunteer Participation

Assessment of the involvement of community volunteers was descriptive rather than strictly analytical. The exploratory nature of this research emphasized flexibility and allowed for community members to both share their local knowledge and receive educational information regarding urban phenology and phenocams. Process notes, including successes and challenges, were kept in detail, and are included in the discussion section of this thesis. Volunteer feedback was also encouraged and recorded when provided so as to better inform the evaluation of methodological efficacy and feasibility.

CHAPTER 4

RESULTS

Phenocam Performance

A total of 15 phenocams remained active for the entire duration of the study period (Table 3).

Table 3. Data collection status for each phenocam. Active status indicates that the phenocam was actively gathering data, while inactive means that the phenocam was no longer collecting data.

Phenocam	SOS 2020	EOS 2020	SOS 2021	EOS 2021	SOS 2022	EOS 2022
Trinidad Ave	Active	Active	Active	Active	Active	Active
17th St.	Active	Active	Active	Active	Inactive	Inactive
First St.	Active	Active	Active	Active	Active	Active
Lang Pl.	Active	Active	Active	Active	Active	Active
A 10th St.	Active	Active	Inactive	Inactive	Inactive	Inactive
A 4th St.	Active	Inactive	Inactive	Inactive	Inactive	Inactive
B 10th St.	Active	Active	Active	Active	Active	Active
B 4th St.	Active	Inactive	Inactive	Inactive	Inactive	Inactive
Delaware Ave		Active	Active	Active	Active	Active
13th St.		Active	Active	Active	Active	Active
California St.		Active	Active	Active	Active	Active
Emerald St.		Active	Active	Active	Active	Active
Q St.		Active	Active	Active	Active	Active
7th St.		Active	Active	Active	Active	Active
F St.		Active	Active	Active	Active	Active
Pershing Dr.		Active	Active	Active	Active	Active
HoS North		Active	Active	Active	Active	Active
HoS South		Active	Active	Active	Active	Active
Kalmia Rd.		Active	Active	Active	Active	Active

The four inactive phenocams were decommissioned over time. Three of the deactivations were the result of volunteer withdrawal and one was due to mechanical failures. Specific mechanical problems included SD card corruption, which affected the storage of data but was fixed with replacement SD cards, and failure to power on, which resulted in the removal of the phenocam. Despite the reduction in phenocams, by the end of the data collection period (EOS 2022), over 270 phenometric estimates were made. The phenocams captured images of a total of 93 trees across 16 genera and 26 species. Of those trees, 47 crowns were identified to the species level and 46 were labeled as “NI”.

Phenological Differences Between Years

Analyses were conducted to determine phenocams’ ability to detect and track differences in phenometrics between years. A one-way ANOVA of the interannual differences in phenometrics yielded a significant F statistic ($F < 0.001$) for SOS, but not for EOS. This suggests that differences in SOS are more easily predicted than differences in EOS and that the source of variance in EOS is likely complex. Given this result, a Tukey’s Honest Significant Difference (HSD) post hoc test was applied to the SOS data (Table 4). The results of the HSD test showed that the years 2020 and 2021 were significantly different from one another, as were 2021 and 2022 ($p < 0.05$).

Table 4. Results of the Tukey's HSD test run for SOS.

Year	Tukey HSD Adjusted p-Value
2020 – 2021	1.81e-4*
2021 - 2022	0.23
2020 - 2022	2.59e-3*

**statistical significance at the 95% level*

The interquartile range (IQR) for each year and phenometric was used to preliminarily look at the spread in the data. SOS IQR decreased from 18 in 2020 to 16 in 2021 and finally 10 in 2022. EOS experienced an increase with 2020 IQR at 25, 2021 at 30, and 2022 at 35. The slight decrease in variability of data distribution in SOS was visualized as a boxplot (Figure 8).

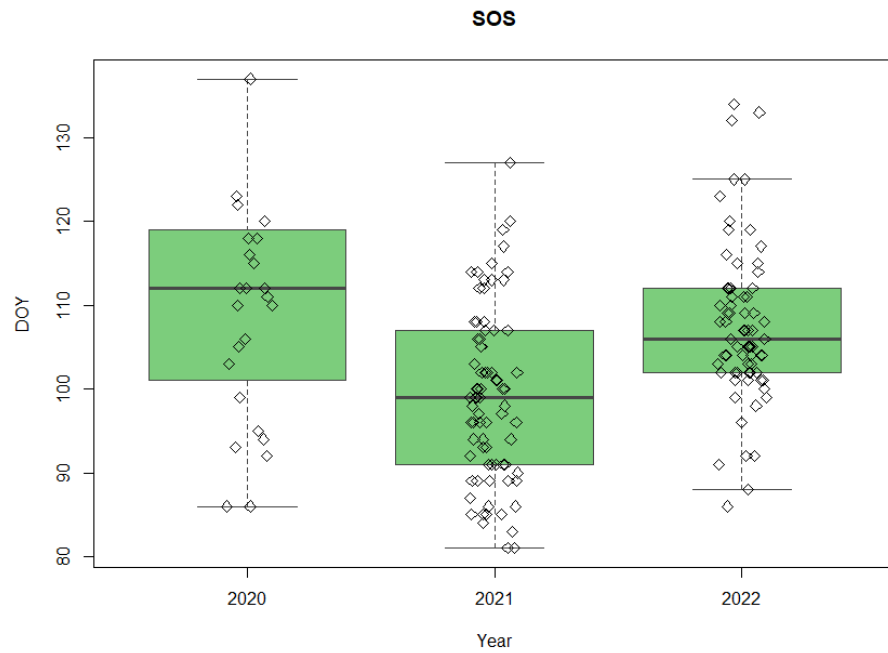


Figure 8. SOS variability by year.

Visual analysis of the SOS boxplot confirmed the significant differences in 2021 SOS.

Many of the trees in 2021 experienced an advance in their SOS. This significant advance may be due to a rapid temperature increase between February 2021 and March 2021 (Figure 9).

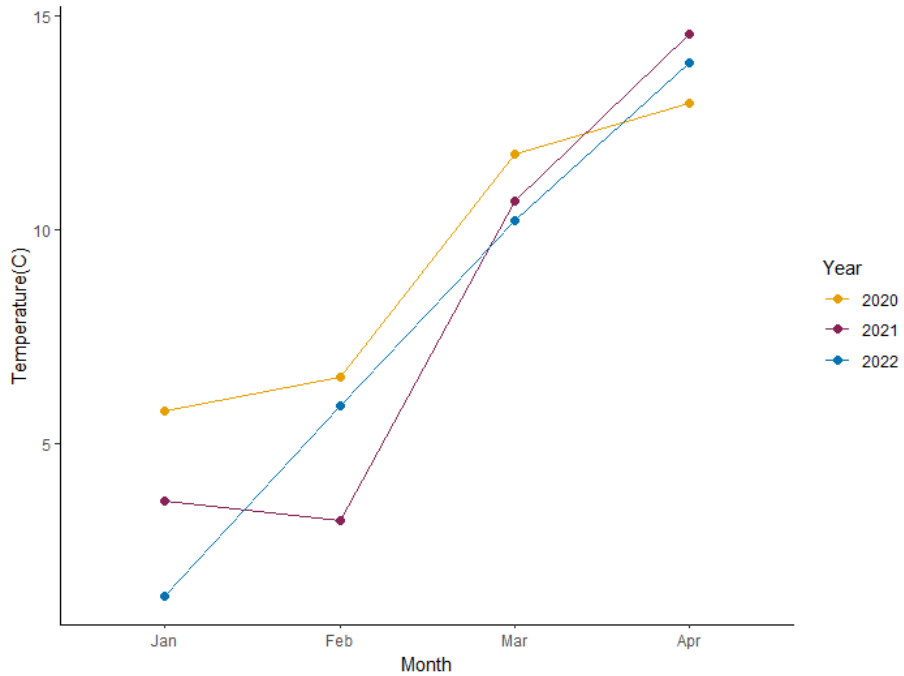


Figure 9. Annual early spring (January – April) temperature averages.

While EOS was not significantly different between years, there were progressive increases in the spread of the EOS values (Figure 10).

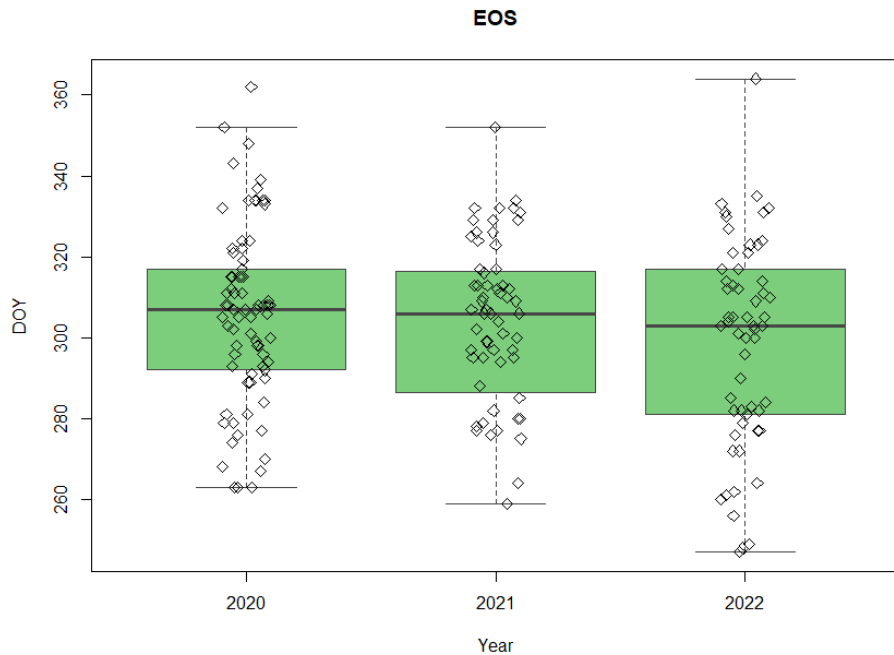


Figure 10. EOS variability by year.

The greater spread of EOS values in 2022 may be attributed to abnormal precipitation patterns during the months leading up to EOS. While 2020 and 2021 experienced high precipitation in the late summer, the 2022 growing season experienced an earlier influx of precipitation in July (Figure 11). The following months were then drier than previous years and may account for the increase in EOS variability among trees.

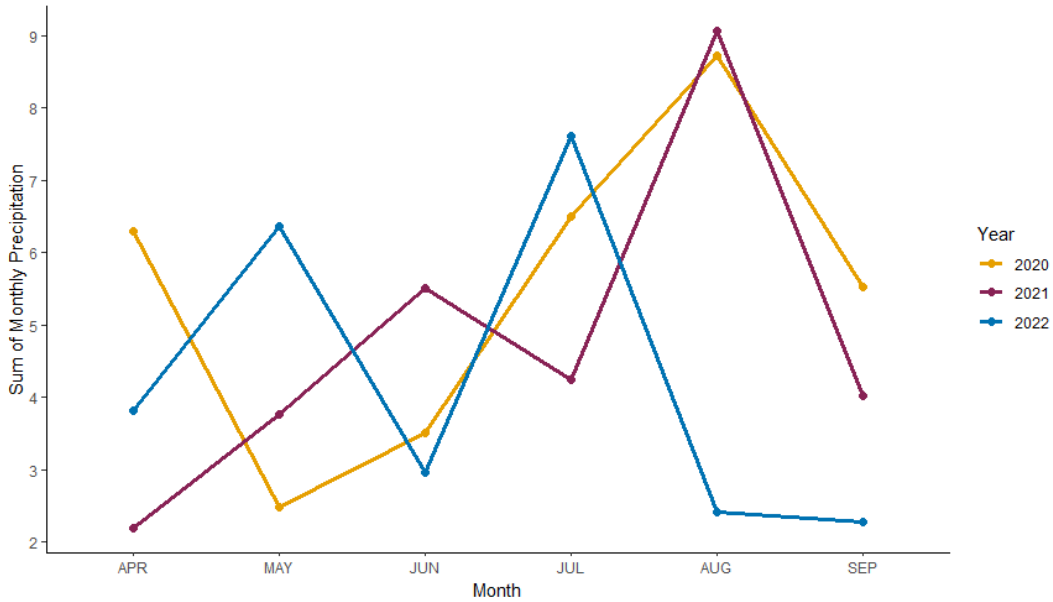


Figure 11. Precipitation sums for the six months preceding EOS for each year.

In addition to analyzing SOS and EOS, a one-way ANOVA found that GSL was significantly different between years as well. Similar to SOS, the years 2020 to 2021 and 2021 to 2022 were significantly different for GSL (Figure 13). Since GSL is a function of both SOS and EOS, it likely responded to the significant differences in SOS.

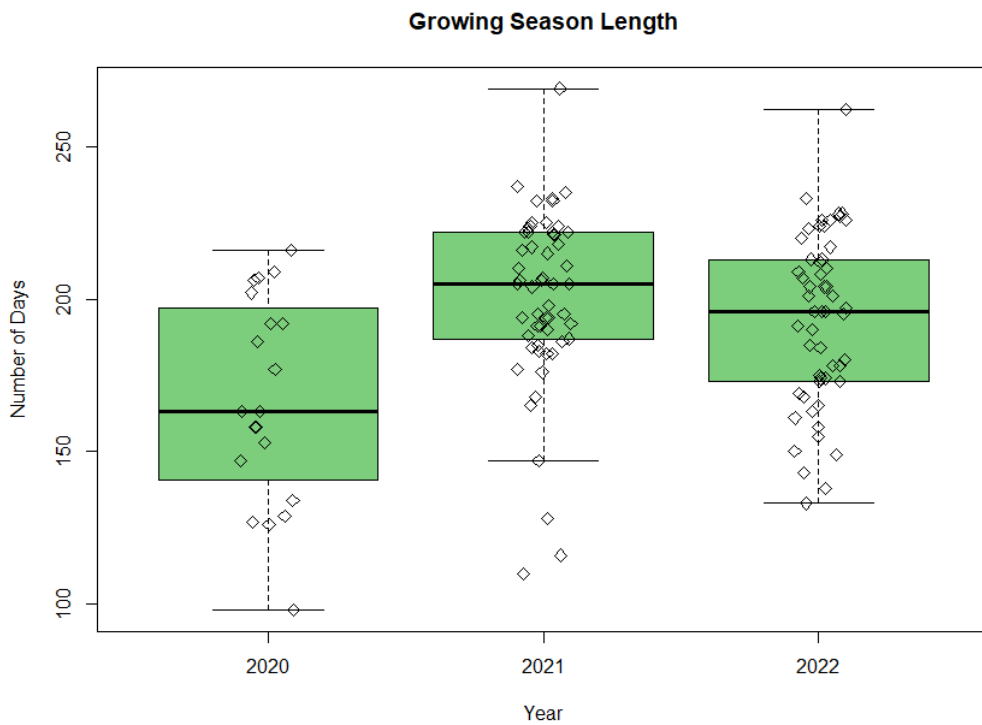


Figure 12. GSL variability by year.

From visual analysis, it is clear that the 2021 growing season was extended compared to the 2020 growing season. Within 2021, there was also far less variability in the data, which indicates that many trees experienced similar GSLs. Within 2022, there was a reduction in the median GSL, as well as an increase in GSL variability.

Hierarchical Mixed Effects Model Outputs

To address objectives in both Aims 1 and 2, hierarchical mixed effects modeling was implemented to determine whether phenocam imagery could capture the relationship between phenology, broad regional climate factors, and local site variables. The models that best fit each phenometric are provided below:

$$SOS = \%IMP + \%TCF + ELEV + TEMP + (1|Phenocam)$$

$$EOS = \%IMP + \%TCF + ELEV + TEMP + PRECIP + (1|Phenocam)$$

Year as a random effect was excluded as it introduced singularity into the regression and interannual differences were better explained by the local or regional variables included in this study. The site variables that were ultimately included in both phenometric models were all associated with the 90-meter buffer. The 90-meter buffer was chosen since it was more representative of the neighborhood around each phenocam. Within the climatic variables, temperatures from the preceding six months of each phenometric yielded the best model results and were therefore included for both SOS and EOS (Table 5). Precipitation, however, did not model SOS well and was excluded from that model. The preceding six-month precipitation sum variable did improve the EOS model, so it was selected.

Table 5. Selected climate variable values representing six-month SOS temperature averages (C°), six-month EOS temperature averages (C°), and six-month precipitation sums for EOS (in.).

Year	SOS TEMP	EOS TEMP	EOS PRECIP
2020	9.23	22.02	33.07
2021	8.63	22.58	33.62
2022	9.02	22.50	25.44

Once the best model for each phenometric was selected through BIC, the RMSE, MAD, and R² values were examined to determine the explanatory power of each model (Table 6).

Table 6. Hierarchical mixed effects model performance indicators.

Model	RMSE	MAD	R ²
SOS	0.88	0.20	0.32
EOS	0.80	0.50	0.38

Final model summaries were produced without standardization so that coefficients could be better interpreted. Non-standardized variable coefficients found that six-month preceding average temperature was significant ($p<0.001$) within the SOS model (Table 7).

Table 7. SOS hierarchical mixed model summary.

	IMP	TCF	ELEV	TEMP
Coefficient	33.12	13.64	-0.06	25.72
Std. Error	60.23	63.82	0.16	9.01
t-value	0.55	0.21	-0.34	2.85
p-value	0.60	0.84	0.71	4.86e-3*

**statistical significance at the 99% level*

No statistical significance was found within the EOS model (Table 8). The negative coefficients (TCF, ELEV, and TEMP) imply that higher canopy cover, elevation, and

temperatures advance EOS phenological events, while the positive coefficients (IMP and PRECIP) indicate that both greater impervious surface cover and precipitation delay EOS.

Table 8. EOS hierarchical mixed model summary.

	IMP	TCF	ELEV	TEMP	PRECIP
Coefficient	78.65	-24.53	-0.01	-0.50	0.21
Std. Error	54.15	53.43	0.14	6.47	0.46
t-value	1.45	-0.46	-0.06	-0.08	0.46
p-value	0.17	0.65	0.96	0.94	0.65

Despite the lack of significant predictor variables in the EOS model, the R^2 value was 0.38, which indicates that 38% of the variance in the data can be explained by the variables (model effects). This R^2 result is likely due to the *phenocam* random effect in the model, highlighting the role of unexplained variability stemming from phenocam placement, care, or other unquantified, site-specific factors.

Ordinary Least Squares Model Outputs

In an attempt to understand the influence of variables without the *phenocam* random effect, OLS regression was used to model SOS and EOS. Like the hierarchical mixed models, OLS models were chosen based on BIC. The final OLS models are provided below:

$$SOS = \%IMP + \%TCF + ELEV + TEMP$$

$$EOS = \%IMP + \%TCF + ELEV + TEMP + PRECIP$$

Both SOS and EOS OLS models included 90-meter site variables and six-month temperature averages. Additionally, precipitation sum of the six months preceding mean EOS was included in the EOS model. Model performance was evaluated using RMSE, MAD, and R² values (Table 9).

Table 9. Ordinary Least Squares model performance indicators.

Model	RMSE	MAD	R ²
SOS	0.98	0.31	0.03
EOS	0.97	0.62	0.04

Upon visual review of fitted and residual plots, potential heteroscedasticity was observed, so the Breusch-Pagan Test for Homoscedasticity was implemented. The test produced the p-values of 0.02 and 0.001 for SOS and EOS respectively. After evaluation, the models were summarized as non-standardized values.

The SOS model produced a significant temperature coefficient (p<0.001) of 17.73 (Table 10). Despite this significant relationship, the R² of the model was low, which indicates that the variables selected for the model do not explain variance in the phenocam data well.

Table 10. SOS OLS model.

	IMP	TEMP	TCF	DTM
Coefficient	-14.94	17.73	9.89	-0.03
Std. Error	12.13	3.97	13.90	0.03
t-value	-1.23	4.47	0.71	-1.10
p-value	0.22	1.45e-05*	0.48	0.28

**statistical significance at 99% level*

Similarly, the R^2 of the EOS model was low, which suggests that EOS variance was also not well explained by the site and climate variables. Of the EOS model climate variables, neither temperature nor precipitation had a significant impact on advancing or delaying the phenometric. Of the site variables, only impervious surface cover was significant ($p<0.05$) with a coefficient of 58.75 (Table 11).

Table 11. EOS OLS model.

	IMP	TEMP	TCF	DTM	PRECIP
Coefficient	58.75	-2.43	5.03	-0.03	0.35
Std. Error	24.90	5.97	25.71	0.05	0.44
t-value	2.36	-0.41	0.20	-0.66	0.76
p-value	0.02*	0.68	0.85	0.51	0.43

**statistical significance at 95% level*

Given that the impervious surface variable was significant within the EOS model, an additional plot was created to examine the relationship between non-standardized impervious surface cover and mean EOS across the different phenocam locations (Figure 13).

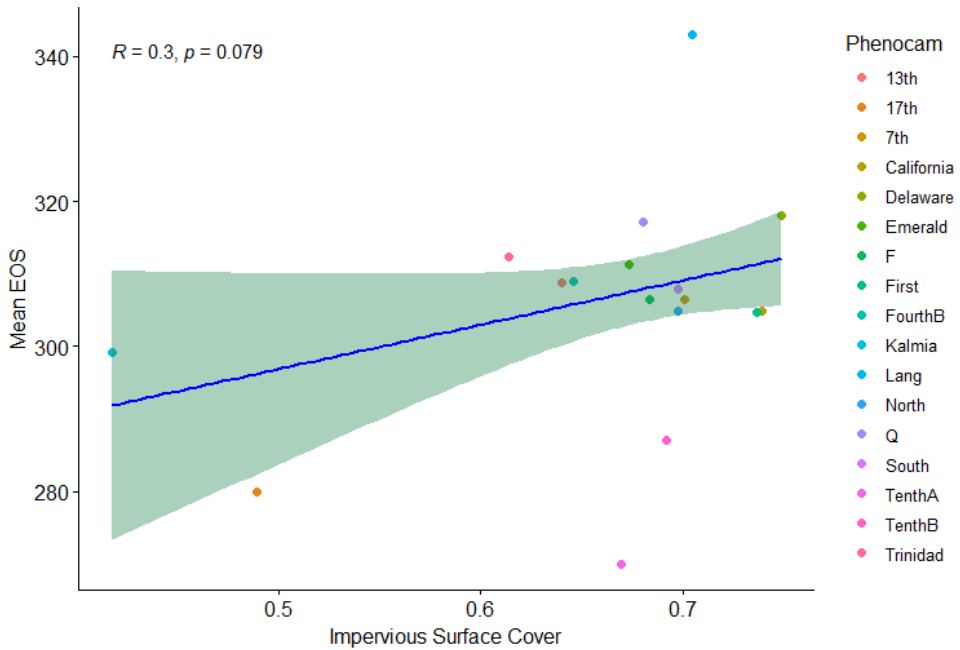


Figure 13. Fractional impervious surface cover by mean EOS. The blue line represents the line of fit and the green area of the plot represents the confidence interval. Data points are colored by phenocam location.

The R value presented in the plot is the correlation coefficient, which serves as a measure of the strength of correlation between impervious surface cover and mean EOS. The p-value included in the plot explains the statistical significance. While the p-value indicates that the correlation between impervious surface and mean EOS is not statistically significant, the correlation coefficient of 0.3 shows that there is a slight positive correlation between the two variables. This result complements the impervious surface result of the OLS EOS model and provides further support for investigating the influence of site factors on urban phenology.

Visualization of Genera Differences

In order to further fulfill the objectives of Aim 2, ANOVAs were performed to determine whether significant differences existed between genera for SOS and EOS data. The ANOVAs

found that SOS differences between genera were not significant, but EOS differences were significant with a p-value of <0.05 . The lack of significant SOS differences in genera implies that external effects, such as planting site or air temperature, are likely obscuring the influence of physiology on the expression of spring phenological responses.

To better compare the variance among the different genera, boxplots of each genera's median phenometric value are provided below (Figures 14 and 15).

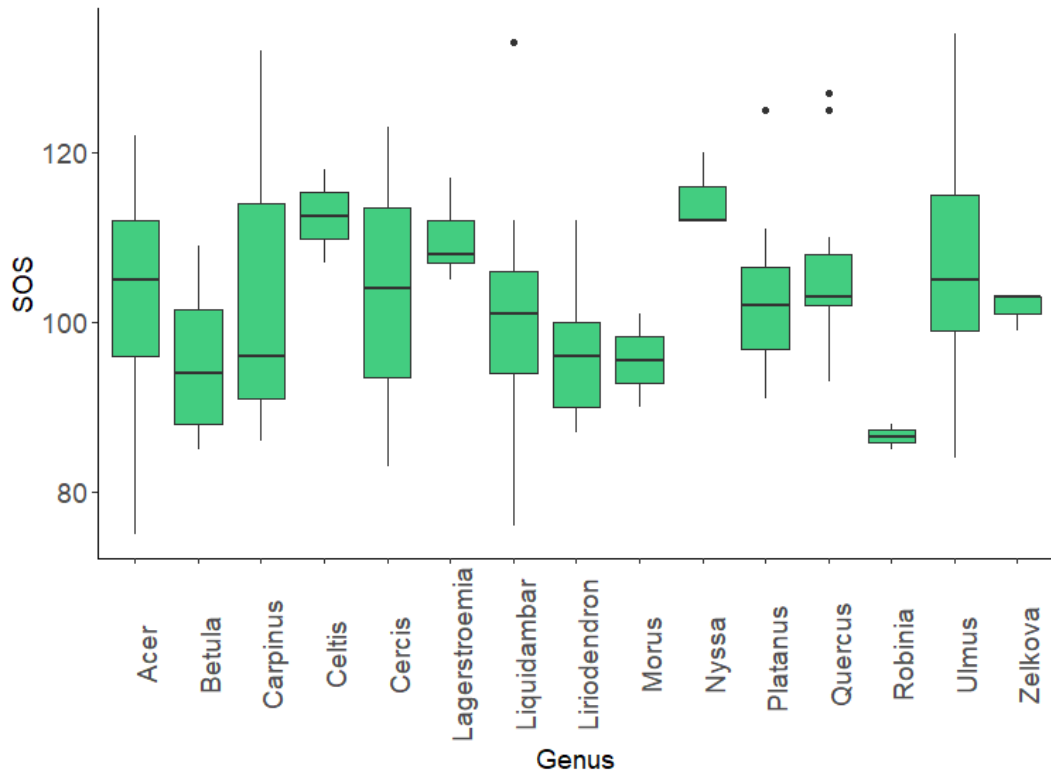


Figure 14. Boxplots of SOS by genus.

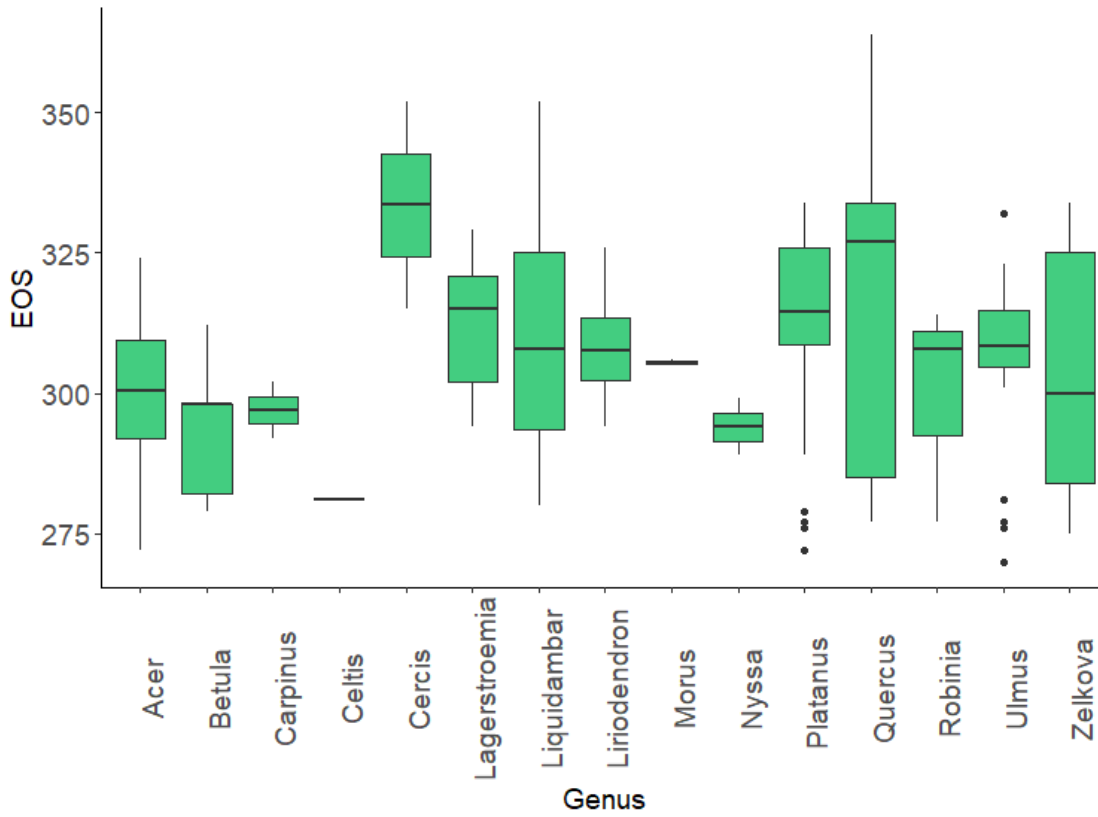


Figure 15. Boxplots of EOS by genus.

Although *genus* was not a statistically significant variable in the modeling of SOS and EOS, differences between genera across years were visualized to examine synchronicity and detect genus-specific trends. The median SOS and EOS values of each genus were plotted against each study year with data grouped and colored by genus (Figures 16 and 17).

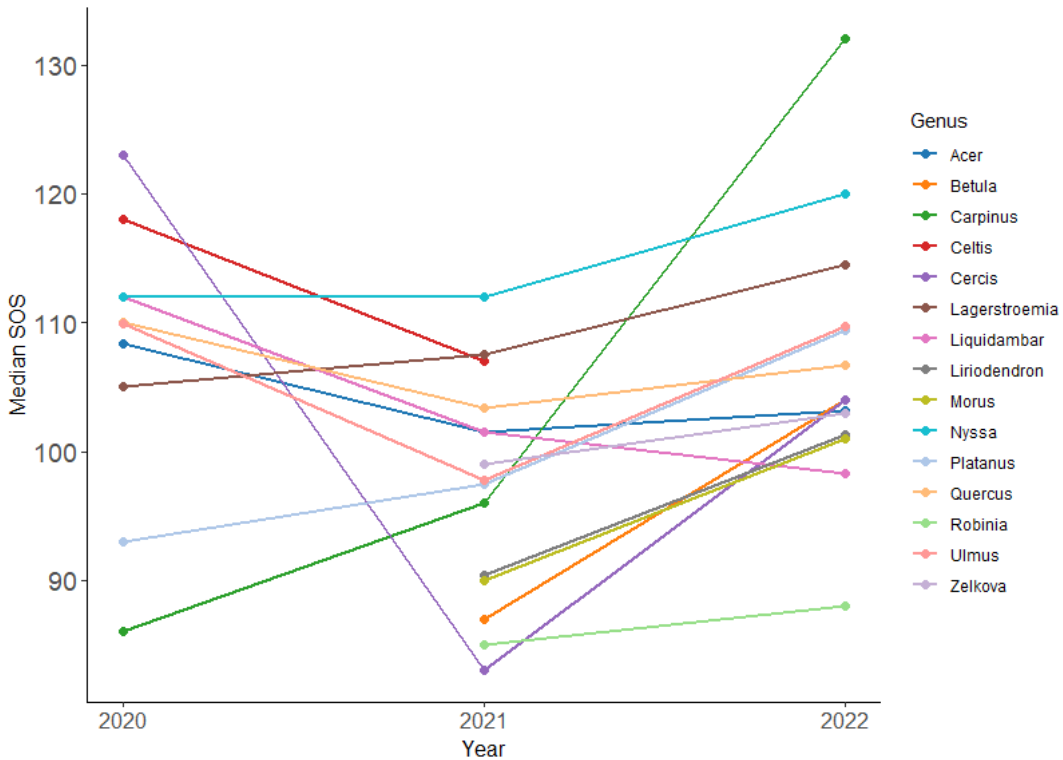


Figure 16. Median SOS plotted against year and colored by genus. Gaps in genera data are produced by missing phenocam data due to phenocam withdrawal, FOV complications, or data loss from technical malfunctions.

Within SOS, there are notable annual shifts in median SOS for many genera. Differences in median SOS from 2020 to 2021 show that four genera experienced a delay in 2021, while five genera advanced the DOY that they experienced SOS. From 2021 to 2022, thirteen genera delayed SOS and only one advanced in SOS. The advancement of SOS indicates that phenological events associated with spring (i.e., bud development and flowering) occurred earlier in the year, while delays in SOS imply that those events began later in the year. These interannual changes disrupted the rank order, or ordered timing, of the genera. Maintenance of genera rank order is important for the timing of other biological or ecological processes within an ecosystem. Changes to the timing of when each genus experiences SOS may suggest the development of greater springtime disruptions.

In EOS, fewer genera experienced large shifts in their median values; however, the genera that did shift tended to do so significantly (Figure 17).

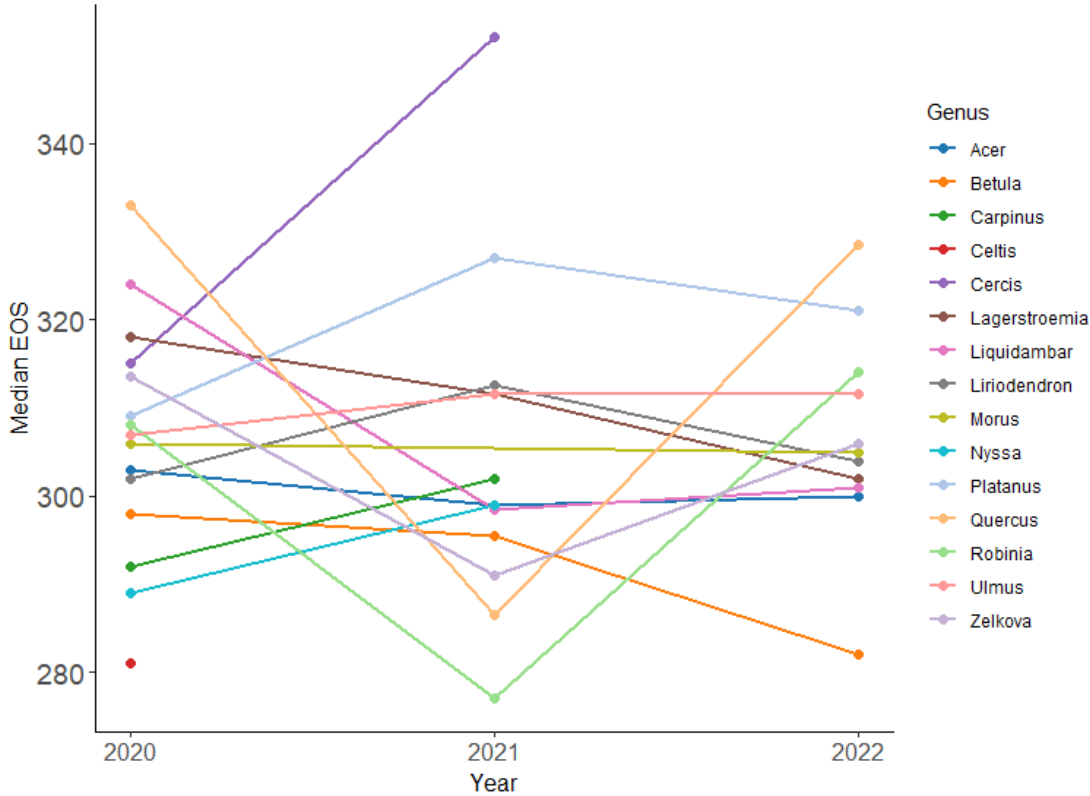


Figure 17. Median EOS plotted against year and colored by genus.

Between 2020 and 2021, six genera advanced their EOS, while seven experienced a delay. Genera such as *Cercis*, *Betula*, and *Carpinus* experienced dramatic changes to their median EOS between the two years. From 2021 to 2022, five of the genera experienced an earlier EOS and four experienced a later EOS. Interestingly, a single genus, *Ulmus*, remained the same from 2021 to 2022 with a median value of DOY 312.

The interannual genera differences in EOS indicate that autumn phenological events like leaf coloring and leaf loss occurred at varying and inconsistent times throughout the study period. High variation in median EOS led to moderate disruption of EOS rank order. Failure to

maintain rank order in EOS reflects the high variability of the summer and autumn effects that govern EOS.

Evaluation of Volunteer Inclusion

In an effort to address Aim 3 of this study, the methodology of using volunteers as phenocam hosts was reviewed both during data collection and post-data collection. Broadly, incorporating volunteers into this urban phenology and phenocam study provided a mix of project benefits and complexities. The primary benefit of the inclusion of community volunteers as phenocam hosts was security for the phenocams. Phenocams were installed on private property with limited access to those not living or working within that private space. Due to this, the risk of phenocam disturbance or unwanted removal was greatly reduced. Additionally, the local knowledge of the volunteers was instrumental in monitoring site changes. For example, volunteers were able to note that one of the study trees had been accidentally sprayed with herbicide, which may have led to the tree's death.

Another important benefit that was gained during the study was the establishment of relationships and connections with a diverse group of local community members. The connection that was created between the study and the volunteers enabled opportunities for educational efforts. For instance, presentations were given at the host-site middle school. These presentations helped increase audience knowledge and provided opportunities for reflection on important background content, methodology, and the broader context of this thesis research. In total, over 160 students and teachers were engaged during two presentations, which expanded the purpose of this thesis to include community engagement.

Crucially, using volunteer homes as hosts for phenocam locations did introduce complexities into the study. Phenocams that were indoors were subject to accidental disturbance depending on their location within the home (e.g., phenocams near frequently opened windows or blinds could be shifted or knocked down). Additionally, large variation in phenocam set-up occurred to accommodate differences in height, angle, and direction of volunteers' canopy view. Such variation was difficult to quantify within this study and consequently introduced excess noise to the phenometric data.

Lastly, some volunteer withdrawal occurred over time. Since access to most of the phenocams was predicated on volunteers being present, any withdrawal of a volunteer resulted in the deactivation of a phenocam. By 2022, three volunteers had withdrawn from the study and had their phenocams collected. The reduction in the number of active phenocams added additional noise to the data but did not overly disrupt the data collection process.

CHAPTER 5

DISCUSSION

Interannual Differences in Phenology

In addressing Aim 1, this study found that phenocams detected slight variation in phenometrics between years. Statistical analysis revealed that only SOS differences between years were significant. In addition, while some variation across years was expected, SOS and EOS did not respond as closely to regional climate, external site, or genera factors as anticipated.

Further examination of the interannual differences in SOS showed that trees in 2021 experienced a large advance in their SOS DOY. This early SOS may be attributed to rapid warming between February and March of 2021. Unlike the other two years, 2021 did not experience a gradual increase in temperature, but rather a quick rise through the month of February into March.

Importantly, the mean February temperature in 2021 was much lower than in 2020 or 2022, which emphasized that sudden increase in temperature and likely signaled trees to begin their spring early. The significant effects of mean air temperature on SOS in this study support previous research that describes air temperature of the months leading up to SOS as highly influential (Menzel 2003, Luo et al. 2006). In addition, this study shows that site conditions can help reasonably track urban phenological change at the individual crown level, which matches with similar results from other studies (Alonzo et al. *accepted*).

Although there were no significant differences found between years for EOS, the variance or spread of the EOS values increased progressively. This may be due in part to large annual variations in precipitation between the months of July, August, and September. Annual

precipitation sums differed both in amount of rainfall and the timing of maximum rainfall between years. In 2020, precipitation increased gradually through the early summer months and peaked in August. Similarly, 2021 precipitation exhibited a similar pattern, but increased and then decreased dramatically around the month of August, which produced a drier September. During 2022, maximum precipitation was lower than in 2020 and 2021. In addition, during the 2022 summer, maximum precipitation occurred much earlier than it had in previous years. This was followed by a period of low precipitation in August and September, which could account for the increase in EOS variance for 2022. Previous studies have found that EOS is sensitive to precipitation shifts such as drought conditions (Xie et al. 2015). Thus, the progressive reduction in precipitation during August and September from 2020 to 2022 likely emphasized differences between tree genera or sites and contributed to EOS variation.

The Effect of Preceding Temperatures on Phenometrics

Modeling the relationship between climate variables and SOS produced significant coefficients for preceding temperature variables. Both the hierarchical mixed effects and OLS models yielded significant positive temperature coefficients. Within the mixed model, the six-month preceding temperature coefficient was positive, which indicates that as temperature increases by one degree, SOS delays by approximately 2.6 days. Similarly, the OLS model generated a positive six-month preceding temperature coefficient that suggests temperature increases of a single degree delay SOS by 1.7 days.

The result of a positive coefficient may be explained by insufficient cold weather during winter months. Deciduous trees in temperate forests need enough cold degree days in the winter

in order to properly break dormancy (Dai et al. 2021). Without these colder temperatures, spring phenology may be altered or delayed (Geng et al. 2020, Man and Dang 2021).

In the Washington, D.C. area, the historic average temperature for December is 5.4°C while the average temperatures for January and February are 3°C and 4.4°C respectively. Combined, the historic average temperature for winter in the D.C. region is approximately 4.3°C (NOAA, n.d.). Within the years of this study, the annual winter temperature averages were higher than historic norms (Figure 18).

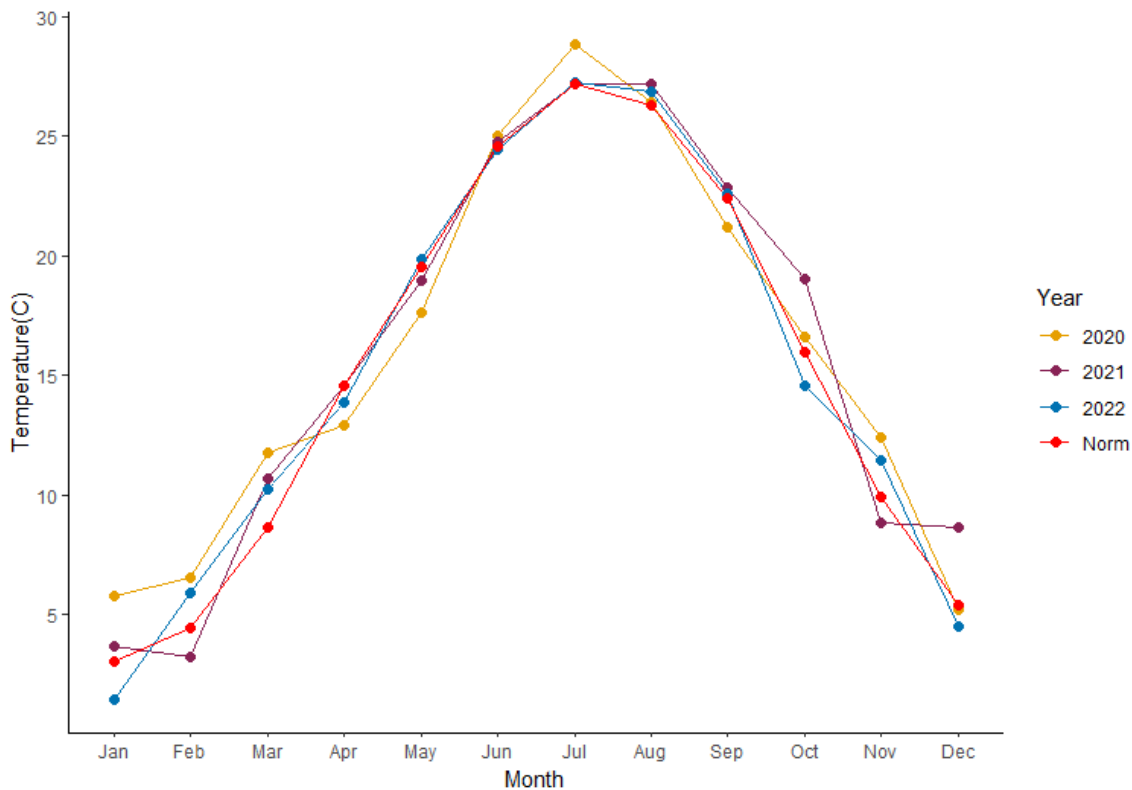


Figure 18. Monthly temperature averages for each study year. The historic average of each month is labeled as "Norm" and colored in bright red.

The warmer winter temperatures likely contributed to variation in SOS values given that there is a diverging relationship between insufficient cold days and higher spring temperatures

(Chuine et al. 1999, Cleland et al. 2007, Fu et al. 2014). While lack of winter chilling may delay trees breaking dormancy, higher preceding spring temperatures may force the start of phenological events.

Unlike SOS, the drivers and mechanisms behind EOS timing are more difficult to ascertain (Cleland et al. 2007, Liu et al. 2016). However, existing literature has found that the timing of EOS phenological events like dormancy are highly influenced by temperature (Menzel 2003, Luo et al. 2006). The temperature coefficients for the EOS mixed effects and OLS models were not significant, but it is worth noting that the coefficients of the six-month preceding temperature averages from both analyses were negative. This indicates that EOS may have advanced under the conditions of higher temperature. The cause of this negative relationship may be partially due to the effect of heat stress on trees.

Heat stress has been shown to force leaf dormancy in certain trees (Xie et al. 2015). In urban environments, trees are subjected to UHI, which exacerbates the heat of summer months (Imhoff et al. 2010, Vogt et al. 2017). When temperatures get too hot, trees tend to prioritize water retention and cooling over photosynthetic activity and may experience leaf mortality during excessive heat days (Teskey et al. 2015). Therefore, it is possible that the increase in temperature, combined with precipitation or drought factors, forced trees to begin EOS events earlier during the study years.

The Effect of Site Variables on Phenology

The only site variable that displayed significance across the models was OLS impervious surface cover for EOS. With a positive coefficient of 58.75, the OLS regression suggests that as impervious surface cover increases by 10%, EOS delays by approximately 5.9 days. This result

supports previous findings that attributed delays in EOS to higher temperatures induced by impervious surfaces and UHI (Mimet et al. 2009, Zipper et al. 2016, Alonzo et al. *accepted*).

Although none of the site variables were significant for SOS, it is worth mentioning that the impervious surface cover displayed the expected relationship of advancing SOS in areas with higher impervious surface cover. This relationship is meaningful as it lends support to potential future studies that aim to investigate phenological shifts in the urban environment.

Genera-Level Differences in Phenometrics

Analysis of SOS and EOS revealed that the two phenometrics are fairly distinct at the genus-level in this study. Unlike trees in rural landscapes, city trees often exist within an artificial or heavily designed plant community (Li et al. 2006). The species that exist in cities are quite often planted and tend to be greatly mixed with native and non-native species (Nitolslawski et al. 2016). In this study, the majority of the genera recorded by phenocams were native, but there were some non-native individuals such as *Zelkova* (elm family) or *Lagerstroemia* (crape myrtle family).

The comparison of median SOS across years for each genus showed that six genera experienced an advance in their 2021 SOS. It is possible that the shift in those six genera could be in response to the fast rise in early spring temperatures that was captured in the preceding six-month temperature variable. Unlike the previous year, which only had a 5.22-degree difference between the months of February and March, the average 2021 March temperature was 7.45 degrees higher than the February average (Table 12).

Table 12. Monthly mean temperatures (C°) for January, February, March, and April of the study period.

Year	Jan	Feb	Mar	Apr
2020	5.78	6.56	11.78	12.94
2021	3.67	3.22	10.67	14.56
2022	1.44	5.89	10.22	13.89

Rank order statistics were not implemented in this study; however, the interannual genera plots were compared with a study that explored individual tree phenology using satellite imagery and performed a similar genera-level visualization as this study (Alonzo et al. *accepted*; Figure 19).

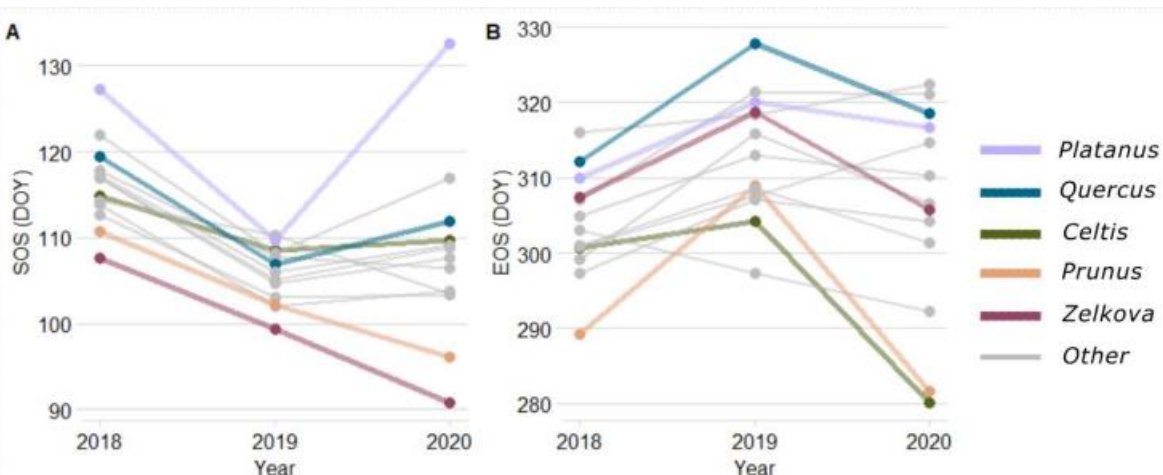


Figure 19. Median phenometric values for each genera plotted across three years. A) SOS, B) EOS (Alonzo et al. *accepted*).

In the prior study, the genera can be seen maintaining rank in SOS. The rank order stability declines slightly in EOS but is still reasonably maintained between years (Alonzo et al. *accepted*). In contrast, the genera of this phenocam study are not clearly maintaining rank order

for either phenometric. This may be a result of the impact that site and climate have on different individuals, or it may be due to additional influences from unquantified effects such as differences in tree care or phenocam angle.

Although the phenocams in this study were able to capture general phenometric change in genera over time, investigation of the specific physiological differences between genera would provide greater insight into the interspecific mechanisms behind changes to phenological responses. For example, other studies that examine differences in phenology across species or genera include variables such as age, height, wood density, or xylem water potential, which provide species or genera-level context for interspecific comparisons (Valdez-Hernández et al. 2010, Basler and Körner 2014, Fréjaville et al. 2019).

Phenocams and Community Science

Phenocams are an affordable, accessible, and customizable tool for gathering data on urban phenology. Using phenocams as the sole method of phenological data collection is relatively novel in urban phenology research. This study aimed to explore the feasibility and utility of using phenocams to collect multi-year phenological data. The study found that the unique benefits associated with this technique include customization of FOV and near-continuous data collection.

Since phenocams can be set up in various locations and at varying angles or heights, it was easy to specifically select canopy rather than concrete, asphalt, or undesirable vegetative matter such as grass. This reduced the chances of obtaining imagery with undesirable targets such bushes or lawns. The FOV was adjustable to each site, which enhanced flexibility in data gathering, but did introduce the potential for FOV shifts over time. Previous phenocam studies

found that small shifts in FOV were generally not an issue, especially when viewing homogenous canopy, but larger shifts required post-collection processing (Richardson et al. 2018).

The near-surface nature of the phenocams allowed for the tracking of phenology at the individual-level, which was extremely useful for capturing phenometric differences between sites and genera. Similarly, the phenocams could be set to collect data at a near-continuous frequency, which allowed for efficient data collection and reduced the time and energy needed to gather a large enough sample size for this study. Similar benefits have been detailed in earlier studies conducted with phenocams (Richardson et al. 2007).

Although this study confirmed the benefits of phenocams, the complexity of working within a city and with battery-powered phenocams was significant. The PhenoCam Network's methodology for installing phenocams recommends placing phenocams at five to ten meters above the canopy, but in urban areas, especially within residential neighborhoods, there are few opportunities for mounting phenocams that high. Similarly, unlike canopy and site conditions in research forests, urban tree and canopy presence varied greatly by site, so the direction and angle of each phenocam was tailored to each site.

Crucially, the phenocams that were used in this study required battery changes approximately every one hundred days. The battery compartment was located on the underside of each phenocam, so it was necessary to disturb the phenocam each time the power source required maintenance. Unfortunately, this often shifted the FOV slightly. Similarly, because some phenocams were attached to indoor windows, if the window opened or was adjusted, or if the suction mount failed, the FOV was subject to shift. To accommodate the variation in FOV,

processing in xROI was tree and FOV-specific. Following this method promoted maximum data preservation.

Additional complexities that were encountered included phenocam damage due to external factors. Though outdoor phenocams were protected in an outer case, some internal failing did occur throughout the study. Moisture was able to enter into some of the outer cases, which caused the batteries to corrode quickly. There were also two instances where SD cards in the phenocams ceased functioning and data were not retrievable. Due to these mechanical challenges, some phenocams stopped working and had to be replaced or removed from the project.

In a prior study that assessed phenocams' ability to track vegetative phenology, three site classes (Type I, II, and III) were created as part of the protocols recommended by the PhenoCam Network (Richardson et al. 2018). These classes are used to describe the locations and set ups of phenocams in participating phenocam projects. The Types refer to the model of phenocam used, as well as set-up and maintenance procedures. Type I phenocam sites use the standard PhenoCam Network protocols, which list a specific brand of camera (NetCam SC IR, StarDot Technologies, Buena Park, CA, USA) and designate maintenance responsibilities to phenocam site hosts. Types II and III describe sites that vary in either the phenocam model or the set-up and maintenance of the phenocam (The PhenoCam Network, n.d.).

Within this urban phenology study, phenocam sites do not fall under any of the previously described Types. The phenocam model that was used in this project was Brinno, which differed from the standard model and brand of the PhenoCam Network. Additionally, each phenocam site required unique set-up conditions, and maintenance was not provided by phenocam volunteer site hosts. Due to these site and study-specific adjustments, phenocam sites

in this research project likely require an additional Type category such as a Type IV. However, to provide better generalization of methods and results, this thesis recommends that future urban phenocam studies use a site class of Type III or lower.

In addition to implementing phenocams, this study engaged community volunteers to act as site hosts. Selected volunteers hosted a phenocam either on a rooftop or on a window. Volunteers did not maintain the equipment but did provide updates or alerts when equipment failed or shifted. Given the source of volunteers, most had a baseline of urban tree knowledge prior to joining the study, but educational conversations and local knowledge were exchanged during each battery-change and data download visit. Presentations were also given at the local middle school hosting one of the phenocams. These presentations provided students with an explanation of the project and a lesson on trees in urban areas. By situating a phenocam at the middle school, and by prioritizing informative conversation during phenocam maintenance, greater community science connections and knowledge were fostered throughout the study period.

Lastly, it is important to note that this study was started prior to the Covid-19 pandemic. Conducting a research project with the help of volunteers during the pandemic made the logistics of accessing the phenocams slightly more complex. Due to this, some volunteers chose to opt out of the study. This did not overly affect data collection; however, it did result in some phenocams being removed from the study. All measures were taken to ensure volunteer and researcher safety during phenocam maintenance visits. Ultimately, the number of active phenocams was influenced by both phenocam malfunction and the withdrawal of volunteers. Due to this, it is recommended that future urban phenocam studies consider the accessibility of phenocam sites, as well as prioritize sites that can remain active for extended periods of time.

CHAPTER 6

CONCLUSION

This novel phenology study explored using phenocams to collect urban phenological data. Modeling climate, site, and genus variables revealed that the only significant climatic variable was the six-month preceding temperature average from the SOS models. Though the relationship between temperature and SOS differed from what was previously expected, lack of cold enough temperatures in the winter months may account for this result. Similarly, the only significant site factor was impervious surface in the EOS OLS model. The relationship between impervious surface and EOS was positive, which supports the expectations of this study, as well as previous findings that show greater impervious surface cover leads to a delay in EOS.

Broadly, the methods applied in this study produced informative and interesting information that both aided in answering the research Aims and provided useful preliminary analyses of urban phenology in D.C. Importantly, the type of phenocam used, as well as the variation in urban study site, created noise in the data, which potentially obscured the strength of relationships between variables and phenometrics. Additionally, the implementation of volunteers likely contributed to unquantifiable variance, which limited the information that could be derived from variable relationships. Despite this, statistical analyses and data visualizations were effective for the general exploration of phenology using phenocams under the conditions of an urban environment.

The phenocams' ability to detect interannual and site phenological differences lend support to their inclusion in future urban phenology research. In addition, this study reinforces the findings of earlier phenocam projects that suggest that phenocams are an accessible tool that can be adapted to suit a variety of study site variations. Ultimately, the findings of this study add

to the existing understanding of urban phenology and provide a foundation for further exploration into using phenocams within cities.

Future research that uses phenocams to obtain urban phenological data would provide great insight into both urban phenology and the technique of implementing phenocams in urban areas. Based on this study, it is recommended that future projects use phenocam set ups that have a connected and continuous power source. Depending on project resources there should be high selectivity regarding the phenocam brand. Although not required, phenocams that capture images in near-infrared would enable better comparisons with satellite imagery products.

Similarly, careful consideration should be taken to ensure that phenocams are protected from inclement weather and disturbance. Secure phenocam sites within cities may be more difficult to obtain, but priority should be given to high, accessible areas that do not experience frequent human traffic. If community volunteers are recruited, then it is recommended that researchers are extremely selective in their choice of location height and phenocam mount. Rooftop sites are recommended, but high indoor windows may also be suitable phenocam installation locations.

Expanding upon the results found in this study, future research into D.C.'s phenology could focus on the influence that physiological differences may have on interannual phenology. Examining physiology would offer additional and testable drivers of phenological differences. Another avenue of focus could include analysis of yearly temperatures preceding a growing season. This may provide greater details about cumulative external influences and the resulting phenological reactions. Finally, future research should include a greater number of phenocams and run the project for an extended length of time to investigate long-term changes and patterns in the phenology of urban trees.

REFERENCES

Aasen, H., Kirchgessner, N., Walter, A., & Liebisch, F. (2020). PhenoCams for Field Phenotyping: Using Very High Temporal Resolution Digital Repeated Photography to Investigate Interactions of Growth, Phenology, and Harvest Traits. *Frontiers in Plant Science*, 11. <https://doi.org/10.3389/fpls.2020.00593>

Alchapar, Noelia L., Correa, Erica N., Cantón, M. Alicia, Classification of building materials used in the urban envelopes according to their capacity for mitigation of the urban heat island in semiarid zones, Energy and Buildings, Volume 69, 2014, Pages 22-32, ISSN 0378-7788, <https://doi.org/10.1016/j.enbuild.2013.10.012>.

Alonso, M., Baker, M., Caplan, J., Williams, A., Elmore, A. (2023) Apparent increase in urban forest growing season length is driven by species and vegetation functional type more than elevated heat. Accepted.

Alonso, M., Baker, M. E., Gao, Y., & Shandas, V. (2021). Spatial configuration and time of day impact the magnitude of urban tree canopy cooling. *Environmental Research Letters*, 16(8). <https://doi.org/10.1088/1748-9326/ac12f2>

Badeck, F.-W., Bondeau, A., Böttcher, K., Doktor, D., Lucht, W., Schabert, J. and Sitch, S. (2004), Responses of spring phenology to climate change. *New Phytologist*, 162: 295-309. <https://doi.org/10.1111/j.1469-8137.2004.01059.x>

Bannari, A., Morin, D., Bonn, F. & Huete, A.R. (1995) A review of vegetation indices, *Remote Sensing Reviews*, 13:1-2, 95-120, DOI: 10.1080/02757259509532298

Basler, David, Körner, Christian. Photoperiod and temperature responses of bud swelling and bud burst in four temperate forest tree species. 2014. 10.1093/treephys/tpu021. *Tree Physiology*. Vol 34. 4. 377. 388. 0829-318X. 7/14/2022.
<https://doi.org/10.1093/treephys/tpu021>

Bloniarz, D.V., Ryan, H.D.P., 1996. The use of volunteer initiatives in conducting urban forest resource inventories. *J. Arboric.* 22, 75–82

Bolton, Gray, J. M., Melaas, E. K., Moon, M., Eklundh, L., & Friedl, M. A. (2020). Continental-scale land surface phenology from harmonized Landsat 8 and Sentinel-2 imagery. *Remote Sensing of Environment*, 240(C), 111685–.
<https://doi.org/10.1016/j.rse.2020.111685>

Browning DM, Karl JW, Morin D, Richardson AD, Tweedie CE. Phenocams Bridge the Gap between Field and Satellite Observations in an Arid Grassland Ecosystem. *Remote Sensing*. 2017; 9(10):1071. <https://doi.org/10.3390/rs9101071>

Casey Trees. *I-Tree Ecosystem Analysis Washington, D.C.* (2015). Retrieved September 1, 2022, from https://caseytrees.org/wp-content/uploads/2017/03/iTree-2015-Report_English.pdf

Chaparro, L., & Terradas, J. (2009). Ecological Services of Urban Forest in Barcelona. Barcelona; Centre de Recerca Ecològica i Aplicacions Forestals.

Chapman, C., K. Valenta, T. M. Bonnell, K. Brown, and L. J. Chapman. 2018. Solar radiation and ENSO predict fruiting phenology patterns in a 15-year record from Kibale National Park, Uganda. *Biotropica* 50: 384– 395.

Chicago Botanic Garden (n.d.). *Budburst: A Project of the Chicago Botanic Garden*. Budburst. Retrieved April 5, 2023, from <https://budburst.org/>

Chmielewski, F., Rötzer, T., Response of tree phenology to climate change across Europe, *Agricultural and Forest Meteorology*, Volume 108, Issue 2, 2001, Pages 101-112, ISSN 0168-1923, [https://doi.org/10.1016/S0168-1923\(01\)00233-7](https://doi.org/10.1016/S0168-1923(01)00233-7).

Chuine, I., Cour, P., & Rousseau, D. D. (1999). Selecting models to predict the timing of flowering of temperate trees: implications for tree phenology modelling. *Plant, Cell and Environment*, 22(1), 1–13. <https://doi.org/10.1046/j.1365-3040.1999.00395.x>

Chuine, I., Belmonte, J., & Mignot, A. (2000). A Modelling Analysis of the Genetic Variation of Phenology between Tree Populations. In *Source: Journal of Ecology* (Vol. 88, Issue 4, pp. 561–570).

Cleland, E. E., Chuine, I., Menzel, A., Mooney, H. A., & Schwartz, M. D. (2007). Shifting plant phenology in response to global change. In *Trends in Ecology and Evolution* (Vol. 22, Issue 7, pp. 357–365). <https://doi.org/10.1016/j.tree.2007.04.003>

Dai, J., Zhu, M., Mao, W., Liu, R., Wang, H., Alatalo, J. M., Tao, Z., & Ge, Q. (2021). Divergent changes of the elevational synchronicity in vegetation spring phenology in North China from 2001 to 2017 in connection with variations in chilling. *International Journal of Climatology*, 41(13), 6109– 6121. <https://doi.org/10.1002/joc.7170>

Davis, Charles C., Lyra, Goia M., Park, Daniel S., Asprino, Renata, Maruyama, Rogério, Torquato, Débora, Cook, Benjamin I., Ellison, Aaron M., New directions in tropical phenology, Trends in Ecology & Evolution, Volume 37, Issue 8, 2022, Pages 683-693, ISSN 0169-5347, <https://doi.org/10.1016/j.tree.2022.05.001>.

Daynes, C. N., Field, D. J., Saleeba, J. A., Cole, M. A., & McGee, P. A. (2013). Development and stabilisation of soil structure via interactions between organic matter, arbuscular mycorrhizal fungi and plant roots. *Soil Biology and Biochemistry*, 57, 683–694. <https://doi.org/10.1016/j.soilbio.2012.09.020>

Dickinson, Janis L., Zuckerberg, Benjamin, Bonter, David N. Citizen Science as an Ecological Research Tool: Challenges and Benefits. 2010. *Annual Review of Ecology, Evolution, and Systematics*. 149-172. V 41. N 1. 10.1146/annurev-ecolsys-102209-144636.

Dunbar, B. (2015, June 16). What is a satellite? NASA. Retrieved August 28, 2022, from <https://www.nasa.gov/audience/forstudents/5-8/features/nasa-knows/what-is-a-satellite-58.html>

Fang, H., Liang, S., Leaf Area Index Models, Reference Module in Earth Systems and Environmental Sciences, Elsevier, 2014, ISBN 9780124095489, <https://doi.org/10.1016/B978-0-12-409548-9.09076-X>.

Ferreira, L.V., Parolin, P. (2007). Tree Phenology In Central Amazonian Floodplain Forests: Effects Of Water Level Fluctuation And Precipitation At Community And Population Level. (Vol. 210, pp. 105–126). Springer Netherlands. https://doi.org/10.1007/978-90-481-8725-6_5

Ford, H., Garbutt, A., Ladd, C., Malarkey, J., & Skov, M. W. (2016). Soil stabilization linked to plant diversity and environmental context in coastal wetlands. *Journal of Vegetation Science*, 27(2), 259–268. <https://doi.org/10.1111/jvs.12367>

Fréjaville, T., Fady, B., Kremer, A., Ducouso, A., & Benito Garzón, M. (2019). Inferring phenotypic plasticity and population responses to climate across tree species ranges using forest inventory data. *Global Ecology and Biogeography*, 28(9), 1259–1271. <https://doi.org/10.1111/geb.12930>

Fritz, S., Fonte, C., & See, L. (2017). The Role of Citizen Science in Earth Observation. *Remote Sensing*, 9(4), 357. MDPI AG. Retrieved from <http://dx.doi.org/10.3390/rs9040357>

Fu, Piao, S., Op de Beeck, M., Cong, N., Zhao, H., Zhang, Y., Menzel, A., & Janssens, I. A. (2014). Recent spring phenology shifts in western Central Europe based on multiscale observations. *Global Ecology and Biogeography*, 23(11), 1255–1263.
<https://doi.org/10.1111/geb.12210>

Geng, Fu, Y. H., Hao, F., Zhou, X., Zhang, X., Yin, G., Vitasse, Y., Piao, S., Niu, K., De Boeck, H. J., Menzel, A., & Peñuelas, J. (2020). Climate warming increases spring phenological differences among temperate trees. *Global Change Biology*, 26(10), 5979–5987.
<https://doi.org/10.1111/gcb.15301>

Gillespie, Alan R, Kahle, Anne B, Walker, Richard E, Color enhancement of highly correlated images. II. Channel ratio and “chromaticity” transformation techniques, *Remote Sensing of Environment*, Volume 22, Issue 3, 1987, Pages 343-365, ISSN 0034-4257,
[https://doi.org/10.1016/0034-4257\(87\)90088-5](https://doi.org/10.1016/0034-4257(87)90088-5).

Graham, Eric A., Riordan, Erin C., Yuen, Eric M., Estrin, Deborah, Rundel, Philip W. (2010). Public internet-connected cameras used as a cross-continental ground-based plant Phenology Monitoring System. *Global Change Biology*. <https://doi.org/10.1111/j.1365-2486.2010.02164.x>

Greene, & Kedron, P. J. (2018). Beyond fractional coverage: A multilevel approach to analyzing the impact of urban tree canopy structure on surface urban heat islands. *Applied Geography* (Sevenoaks), 95, 45–53. <https://doi.org/10.1016/j.apgeog.2018.04.004>

Günter, S., Stimm, B., Cabrera, M., Diaz, M., Lojan, M., Ordoñez, E., . . . Weber, M. (2008). Tree phenology in montane forests of southern Ecuador can be explained by precipitation, radiation and photoperiodic control. *Journal of Tropical Ecology*, 24(3), 247-258. doi:10.1017/S0266467408005063

Imhoff, M. L., Zhang, P., Wolfe, R. E., & Bounoua, L. (2010). Remote sensing of the urban heat island effect across biomes in the continental USA. *Remote Sensing of Environment*, 114(3), 504–513. <https://doi.org/10.1016/j.rse.2009.10.008>

Inoue, T., Nagai, S., Kobayashi, H., et al. Utilization of ground-based digital photography for the evaluation of seasonal changes in the aboveground green biomass and foliage phenology in a grassland ecosystem. *Ecol. Inform.*, 25 (2015), pp. 1-9

Jin, H., Jönsson, A.M., Olsson, C. et al. New satellite-based estimates show significant trends in spring phenology and complex sensitivities to temperature and precipitation at northern

European latitudes. *Int J Biometeorol* 63, 763–775 (2019).
<https://doi.org/10.1007/s00484-019-01690-5>

Jochner, S., & Menzel, A. (2015). Urban phenological studies - Past, present, future. In *Environmental Pollution* (Vol. 203, pp. 250–261). Elsevier Ltd.
<https://doi.org/10.1016/j.envpol.2015.01.003>

Jochner, S.C., Sparks, T.H., Estrella, N. et al. The influence of altitude and urbanisation on trends and mean dates in phenology (1980–2009). *Int J Biometeorol* 56, 387–394 (2012).
<https://doi.org/10.1007/s00484-011-0444-3>

Kabano, P., Harris, A., & Lindley, S. (2021). Sensitivity of Canopy Phenology to Local Urban Environmental Characteristics in a Tropical City. *Ecosystems*, 24(5), 1110–1124.
<https://doi.org/10.1007/s10021-020-00571-y>

Kalusova, Ceplova, N., & Lososova, Z. (2017). Which traits influence the frequency of plant species occurrence in urban habitat types? *Urban Ecosystems*, 20(1), 65–75.
<https://doi.org/10.1007/s11252-016-0588-3>

Kosmala, M., Crall, A., Cheng, R., Hufkens, K., Henderson, S., & Richardson, A. (2016). Season Spotter: Using Citizen Science to Validate and Scale Plant Phenology from Near-Surface Remote Sensing. *Remote Sensing*, 8(9), 726. MDPI AG. Retrieved from <http://dx.doi.org/10.3390/rs8090726>

Kirschbaum, M.U.F. Can Trees Buy Time? An Assessment of the Role of Vegetation Sinks as Part of the Global Carbon Cycle. *Climatic Change* 58, 47–71 (2003).
<https://doi.org/10.1023/A:1023447504860>

Koenig, Knops, J. M. H., Carmen, W. J., & Pearse, I. S. (2015). What drives masting? The phenological synchrony hypothesis. *Ecology* (Durham), 96(1), 184–192.
<https://doi.org/10.1890/14-0819.1>

Landsberg, Helmut E., The Urban Climate, International Geophysics, Academic Press, Volume 28, 1981, ISSN 0074-6142, ISBN 9780124359604, [https://doi.org/10.1016/S0074-6142\(08\)60183-7](https://doi.org/10.1016/S0074-6142(08)60183-7).

Letter, C., Jäger, G. Simulating the potential of trees to reduce particulate matter pollution in urban areas throughout the year. *Environ Dev Sustain* 22, 4311–4321 (2020).
<https://doi.org/10.1007/s10668-019-00385-6>

Li, W., Ouyang, Z., Meng, X., & Wang, X. (2006). Plant species composition in relation to green cover configuration and function of urban parks in Beijing, China. *Ecological Research*, 21(2), 221–237. <https://doi.org/10.1007/s11284-005-0110-5>

Li, X., & Ratti, C. (2018, March 6). Mapping the spatial distribution of shade provision of street trees in Boston using google street view panoramas. *Urban Forestry & Urban Greening*.

Liang, L., Schwartz, M.D. & Fei, S. Photographic assessment of temperate forest understory phenology in relation to springtime meteorological drivers. *Int J Biometeorol* 56, 343–355 (2012). <https://doi.org/10.1007/s00484-011-0438-1>

Liu, Q., Fu, Y.H., Zhu, Z., Liu, Y., Liu, Z., Huang, M., Janssens, I.A. and Piao, S. (2016), Delayed autumn phenology in the Northern Hemisphere is related to change in both climate and spring phenology. *Glob Change Biol*, 22: 3702-3711. <https://doi.org/10.1111/gcb.13311>

Los, S. O., Pollack, N. H., Parris, M. T., Collatz, G. J., Tucker, C. J., Sellers, P. J., Malmström, C. M., DeFries, R. S., Bounoua, L., & Dazlich, D. A. (2000). A Global 9-yr Biophysical Land Surface Dataset from NOAA AVHRR Data, *Journal of Hydrometeorology*, 1(2), 183-199. Retrieved Mar 5, 2023.

Luo, Z., Sun, O.J., Ge, Q. et al. Phenological responses of plants to climate change in an urban environment. *Ecol Res* 22, 507–514 (2007). <https://doi.org/10.1007/s11284-006-0044-6>

Man, Lu, P., & Dang, Q.-L. (2021). Effects of insufficient chilling on budburst and growth of six temperate forest tree species in Ontario. *New Forests*, 52(2), 303–315. <https://doi.org/10.1007/s11056-020-09795-1>

Mayor, S.J., Guralnick, R.P., Tingley, M.W. et al. Increasing phenological asynchrony between spring green-up and arrival of migratory birds. *Sci Rep* 7, 1902 (2017). <https://doi.org/10.1038/s41598-017-02045-z>

McGrath, L. J., van Riper, C., & Fontaine, J. J. (2009). Flower Power: Tree Flowering Phenology as a Settlement Cue for Migratory Birds. *Journal of Animal Ecology*, 78(1), 22–30. <http://www.jstor.org/stable/27696337>

McKinley, D. C., Miller-Rushing, A. J., Ballard, H. L., Bonney, R., Brown, H., Cook-Patton, S. C., Evans, D. M., French, R. A., Parrish, J. K., Phillips, T. B., Ryan, S. F., Shanley, L. A., Shirk, J. L., Stepenuck, K. F., Weltzin, J. F., Wiggins, A., Boyle, O. D., Briggs, R. D., Chapin, S. F., Soukup, M. A. (2017). Citizen science can improve conservation science, natural resource management, and environmental protection. *Biological Conservation*, 208, 15–28. <https://doi.org/10.1016/j.biocon.2016.05.015>

Meier, I.C., Leuschner, C. & Hertel, D. Nutrient return with leaf litter fall in *Fagus sylvatica* forests across a soil fertility gradient. *Plant Ecol* 177, 99–112 (2005).
<https://doi.org/10.1007/s11258-005-2221-z>

Melaas, E. K., Friedl, M. A., & Zhu, Z. (2013). Detecting interannual variation in deciduous broadleaf forest phenology using Landsat TM/ETM+ data. *Remote Sensing of Environment*, 132, 176–185. <https://doi.org/10.1016/j.rse.2013.01.011>

Melaas, E. K., Wang, J. A., Miller, D. L., & Friedl, M. A. (2016). Interactions between urban vegetation and surface urban heat islands: A case study in the Boston metropolitan region. *Environmental Research Letters*, 11(5). <https://doi.org/10.1088/1748-9326/11/5/054020>

Menzel, A., Fabian, P. Growing season extended in Europe. *Nature* 397, 659 (1999).
<https://doi.org/10.1038/17709>

Menzel, A. (2003) Plant phenological anomalies in Germany and their relation to air temperature and NAO. *Climatic Change* 57, 243–263

Mimet, Pellissier, V., Quénol, H., Aguejjad, R., Dubreuil, V., & Rozé, F. (2009). Urbanisation induces early flowering: evidence from *Platanus acerifolia* and *Prunus cerasus*. *International Journal of Biometeorology*, 53(3), 287–298. <https://doi.org/10.1007/s00484-009-0214-7>

Miri, A., Davidson-Arnott, R. (2021). The effectiveness of a single *Tamarix* tree in reducing aeolian erosion in an arid region. *Agricultural and Forest Meteorology*, 300, 108324. <https://doi.org/10.1016/j.agrformet.2021.108324>

Molinier, M., López-Sánchez, C., Toivanen, T., Korpela, I., Corral-Rivas, J., Terguieff, R., & Häme, T. (2016). Relasphone—Mobile and Participative In Situ Forest Biomass Measurements Supporting Satellite Image Mapping. *Remote Sensing*, 8(10), 869. MDPI AG. Retrieved from <http://dx.doi.org/10.3390/rs8100869>

Moon, Li, D., Liao, W., Rigden, A. J., & Friedl, M. A. (2020). Modification of surface energy balance during springtime: The relative importance of biophysical and meteorological changes. *Agricultural and Forest Meteorology*, 284, 107905.
<https://doi.org/10.1016/j.agrformet.2020.107905>

Morin, Xavier, Lechowicz, Martin J., Augspurger, Carol, O'keefe, John, Viner, David, Chuine, Isabelle. (2009). Leaf phenology in 22 North American tree species during the 21st century. *Global Change Biology*, 15(4), 961–975. <https://doi.org/10.1111/j.1365-2486.2008.01735.x>

Nagai, S., Ichie, T., Yoneyama, A., et al. Usability of time-lapse digital camera images to detect characteristics of tree phenology in a tropical rainforest. *Ecol. Inform.*, 32 (2016), pp. 91–106

National Oceanic and Atmospheric Administration (NOAA) (n.d.). *Climate*. National Weather Service. Retrieved January 27, 2023, from
<https://www.weather.gov/wrh/Climate?wfo=lwx>

Nitoslawski, Duinker, P. N., & Bush, P. G. (2016). A review of drivers of tree diversity in suburban areas: Research needs for North American cities. *Environmental Reviews*, 24(4), 471–483. <https://doi.org/10.1139/er-2016-0027>

Nowak, D., Hoehn, R., & Crane, D. (2007). Oxygen production by urban trees in the United States. *Arboriculture & Urban Forestry*, 33(3), 220–226.
<https://doi.org/10.48044/jauf.2007.026>

Pellerin, M., Delestrade, A., Mathieu, G. et al. Spring tree phenology in the Alps: effects of air temperature, altitude and local topography. *Eur J Forest Res* 131, 1957–1965 (2012).
<https://doi.org/10.1007/s10342-012-0646-1>

Peters, Valerie E., Carlo, Tomás A., Mello, Marco A. R., Rice, Robert A., Tallamy, Doug W., Caudill, Amanda S., Fleming, Theodore H., Using Plant–Animal Interactions to Inform Tree Selection in Tree-Based Agroecosystems for Enhanced Biodiversity, *BioScience*, Volume 66, Issue 12, December 2016, Pages 1046–1056,
<https://doi.org/10.1093/biosci/biw140>

Polgar, C., Gallinat, A., & Primack, R. B. (2013). Drivers of leaf-out phenology and their implications for species invasions: Insights from Thoreau's Concord. *New Phytologist*, 202(1), 106–115. <https://doi.org/10.1111/nph.12647>

Prevedello, J. A., Almeida-Gomes, M., & Lindenmayer, D. B. (2017). The importance of scattered trees for biodiversity conservation: A global meta-analysis. *Journal of Applied Ecology*, 55(1), 205–214. <https://doi.org/10.1111/1365-2664.12943>

Reed, B. C., Brown, J. F., VanderZee, D., Loveland, T. R., Merchant, J. W., & Ohlen, D. O. (1994). Measuring phenological variability from satellite imagery. *Journal of Vegetation Science*, 5(5), 703–714. <https://doi.org/10.2307/3235884>

Reid, Anya M., Chapman, William K., Prescott, Cindy E., Nijland, Wiebe, Using excess greenness and green chromatic coordinate colour indices from aerial images to assess lodgepole pine vigour, mortality and disease occurrence, *Forest Ecology and Management*, Volume 374, 2016, Pages 146-153, ISSN 0378-1127, <https://doi.org/10.1016/j.foreco.2016.05.006>.

Richardson, A. D., Hufkens, K., Milliman, T., Aubrecht, D. M., Chen, M., Gray, J. M., Johnston, M. R., Keenan, T. F., Klosterman, S. T., Kosmala, M., Melaas, E. K., Friedl, M. A., & Frolking, S. (2018). Tracking vegetation phenology across diverse North American biomes using PhenoCam imagery. *Scientific Data*, 5. <https://doi.org/10.1038/sdata.2018.28>

Richardson, A.D., Hufkens, K., Milliman, T. et al. Intercomparison of phenological transition dates derived from the PhenoCam Dataset V1.0 and MODIS satellite remote sensing. *Sci Rep* 8, 5679 (2018). <https://doi.org/10.1038/s41598-018-23804-6>

Richardson, A. D., Jenkins, J. P., Braswell, B. H., Hollinger, D. Y., Ollinger, S. v., & Smith, M. L. (2007). Use of digital webcam images to track spring green-up in a deciduous broadleaf forest. *Oecologia*, 152(2), 323–334. <https://doi.org/10.1007/s00442-006-0657-z>

Richardson, A. D., Andy Black, T., Ciais, P., Delbart, N., Friedl, M. A., Gobron, N., Hollinger, D. Y., Kutsch, W. L., Longdoz, B., Luyssaert, S., Migliavacca, M., Montagnani, L., William Munger, J., Moors, E., Piao, S., Rebmann, C., Reichstein, M., Saigusa, N., Tomelleri, E., ... Varlagin, A. (2010). Influence of spring and autumn phenological transitions on forest ecosystem productivity. *Philosophical Transactions of the Royal Society B: Biological Sciences*, 365(1555), 3227–3246. <https://doi.org/10.1098/rstb.2010.0102>

Roman, L. A., Mcpherson, E. G., Scharenbroch, B. C., & Bartens, J. (n.d.). *Roman et al: Common Practices and Challenges for Urban Tree Monitoring Programs Identifying*

Common Practices and Challenges for Local Urban Tree Monitoring Programs Across the United States.

Roman, L. A., Scharenbroch, B. C., Östberg, J. P. A., Mueller, L. S., Henning, J. G., Koeser, A. K., Sanders, J. R., Betz, D. R., & Jordan, R. C. (2017). Data quality in citizen science urban tree inventories. *Urban Forestry and Urban Greening*, 22, 124–135.
<https://doi.org/10.1016/j.ufug.2017.02.001>

Rosemartin, A., Watkins, T., & Miller-Rushing, A. J. (2021). Monitoring phenology in US national parks through citizen science: Some preliminary lessons and prospects for protected areas. *Parks Stewardship Forum*, 37(3). <http://dx.doi.org/10.5070/P537354739>
Retrieved from <https://escholarship.org/uc/item/55s215mx>

Sabrin, S., Karimi, M., Nazari, R., Pratt, J., & Bryk, J. (2020, December 29). Effects of different urban-vegetation morphology on the canopy-level thermal comfort and the cooling benefits of shade trees: Case-study in Philadelphia. *Sustainable Cities and Society*.

Schaber, J., Badeck, F.W. Physiology-based phenology models for forest tree species in Germany. *Int J Biometeorol* 47, 193–201 (2003). <https://doi.org/10.1007/s00484-003-0171-5>

Seyednasrollah, Young, A. M., Hufkens, K., Milliman, T., Friedl, M. A., Froliking, S., & Richardson, A. D. (2019). Tracking vegetation phenology across diverse biomes using Version 2.0 of the PhenoCam Dataset. *Scientific Data*, 6(1), 222–11.
<https://doi.org/10.1038/s41597-019-0229-9>

Seyednasrollah, B. (2022). Delineate Region of Interests (ROI's) and Extract Time-Series Data from Digital Repeat Photography Images. Package ‘xROI’. Version 0.9.20. <https://cran.r-project.org/web/packages/xROI/xROI.pdf>

Shandas, V., Voelkel, J., Williams, J., & Hoffman, J. (2019). Integrating Satellite and Ground Measurements for Predicting Locations of Extreme Urban Heat. *Climate*, 7(1), 5. MDPI AG. Retrieved from <http://dx.doi.org/10.3390/cli7010005>

Shukla, A., & Srivastava, S. (2019). A review of phytoremediation prospects for arsenic contaminated water and soil. *Phytomanagement of Polluted Sites*, 243–254.
<https://doi.org/10.1016/b978-0-12-813912-7.00008-9>

Schwartz, Mark & Reiter, Bernhard. (2000). Changes in North American spring. *International Journal of Climatology*. 20. 929-932. 10.1002/1097-0088(20000630)20:8%3C929::AID-JOC557%3E3.0.CO;2-5.

Solomon, A.M. (1997). Natural migration rates of trees: Global terrestrial carbon cycle implications. In: Huntley, B., Cramer, W., Morgan, A.V., Prentice, H.C., Allen, J.R.M. (eds) *Past and Future Rapid Environmental Changes*. NATO ASI Series, vol 47. Springer, Berlin, Heidelberg. https://doi.org/10.1007/978-3-642-60599-4_35

Song, P., Sexton, J.O., Huang, C., Channan, S., Townshend, J.R. (2016). Characterizing the magnitude, timing and duration of urban growth from time series of Landsat-based estimates of impervious cover, *Remote Sensing of Environment*, Volume 175, Pages 1-13, ISSN 0034-4257, <https://doi.org/10.1016/j.rse.2015.12.027>.

Sonnentag, O., Hufkens, K., Teshera-Sterne, C., Young, A. M., Friedl, M., Braswell, B. H., Milliman, T., O'Keefe, J., & Richardson, A. D. (2012). Digital repeat photography for phenological research in forest ecosystems. *Agricultural and Forest Meteorology*, 152(1), 159–177. <https://doi.org/10.1016/j.agrformet.2011.09.009>

Southwood, Richard, Wint, T.E., Kennedy, G.R. C. E. J., Greenwood, S.R. (2005). The composition of the arthropod fauna of the canopies of some species of oak (*Quercus*). *European Journal of Entomology*, 102(1), 65–72. <https://doi.org/10.14411/eje.2005.009>

Stagoll, K., Lindenmayer, D. B., Knight, E., Fischer, J., & Manning, A. D. (2012). Large trees are keystone structures in Urban parks. *Conservation Letters*, 5(2), 115–122. <https://doi.org/10.1111/j.1755-263x.2011.00216.x>

Studer, S., Stöckli, R., Appenzeller, C. et al. A comparative study of satellite and ground-based phenology. *Int J Biometeorol* 51, 405–414 (2007). <https://doi.org/10.1007/s00484-006-0080-5>

Teets, Bailey, A. S., Hufkens, K., Ollinger, S., Schädel, C., Seyednasrollah, B., & Richardson, A. D. (2023). Early spring onset increases carbon uptake more than late fall senescence: modeling future phenological change in a US northern deciduous forest. *Oecologia*, 201(1), 241–257. <https://doi.org/10.1007/s00442-022-05296-4>

Teskey, Wertin, T., Bauweraerts, I., Ameye, M., McGuire, M. A., & Steppe, K. (2015). Responses of tree species to heat waves and extreme heat events: Tree response to extreme heat. *Plant, Cell and Environment*, 38(9), 1699–1712. <https://doi.org/10.1111/pce.12417>

The European Space Agency (ESA) (n.d.). *Resolutions*. Sentinel Online. Retrieved January 15, 2023, from <https://sentinels.copernicus.eu/web/sentinel/user-guides/sentinel-2-msi/resolutions#:~:text=The%20resolutions%20of%20the%20SENTINEL,constellation%20revisit%20is%205%20days>.

The National Aeronautics and Space Administration (NASA) (n.d.). *Terra & Aqua Moderate Resolution Imaging Spectroradiometer (MODIS)*. LAADS DAAC. Retrieved January 15, 2023, from <https://ladsweb.modaps.eosdis.nasa.gov/missions-and-measurements/modis/>

The PhenoCam Network. (n.d.). Retrieved September 1, 2022, from <https://phenocam.nau.edu/webcam/education/>

Theobald, E. J., Ettinger, A. K., Burgess, H. K., DeBey, L. B., Schmidt, N. R., Froehlich, H. E., Wagner, C., HilleRisLambers, J., Tewksbury, J., Harsch, M. A., & Parrish, J. K. (2015). Global change and local solutions: Tapping the unrealized potential of citizen science for biodiversity research. *Biological Conservation*, 181, 236–244. <https://doi.org/10.1016/j.biocon.2014.10.021>

Threlfall, C. G., Mata, L., Mackie, J. A., Hahs, A. K., Stork, N. E., Williams, N. S., & Livesley, S. J. (2017). Increasing biodiversity in urban green spaces through simple vegetation interventions. *Journal of Applied Ecology*, 54(6), 1874–1883. <https://doi.org/10.1111/1365-2664.12876>

Townshend, J.R.G. and Justice, C.O. 1988. Selecting the spatial resolution of satellite sensors required for global monitoring of land transformations. *International Journal of Remote Sensing*, 9: 187–236.

Townshend, J. R., Masek, J. G., Huang, C., Vermote, E. F., Gao, F., Channan, S., Sexton, J. O., Feng, M., Narasimhan, R., Kim, D., Song, K., Song, D., Song, X.-P., Noojipady, P., Tan, B., Hansen, M. C., Li, M., & Wolfe, R. E. (2012). Global characterization and monitoring of forest cover using Landsat Data: Opportunities and challenges. *International Journal of Digital Earth*, 5(5), 373–397. <https://doi.org/10.1080/17538947.2012.713190>

Tscharntke, T., Clough, Y., Bhagwat, S. A., Buchori, D., Faust, H., Hertel, D., Hölscher, D., Juhrbandt, J., Kessler, M., Perfecto, I., Scherber, C., Schroth, G., Veldkamp, E., & Wanger, T. C. (2011). Multifunctional shade-tree management in tropical agroforestry landscapes - A Review. *Journal of Applied Ecology*, 48(3), 619–629. <https://doi.org/10.1111/j.1365-2664.2010.01939.x>

United Census Bureau (2022, September 16). 2020 Census Results. United States Government. Retrieved July 21, 2022, from <https://www.census.gov/programs-surveys/decennial-census/decade/2020/2020-census-results.html>

USA National Phenology Network (n.d.). *Nature's Notebook*. Nature's Notebook | USA National Phenology Network. Retrieved April 5, 2023, from https://www.usanpn.org/natures_notebook

Vailshery, Jaganmohan, M., & Nagendra, H. (2013). Effect of street trees on microclimate and air pollution in a tropical city. *Urban Forestry & Urban Greening*, 12(3), 408–415. <https://doi.org/10.1016/j.ufug.2013.03.002>

Valdez-Hernández, M., Andrade, J.L., Jackson, P.C. et al. Phenology of five tree species of a tropical dry forest in Yucatan, Mexico: effects of environmental and physiological factors. *Plant Soil* 329, 155–171 (2010). <https://doi.org/10.1007/s11104-009-0142-7>

Vitasse, Y., Porté, A.J., Kremer, A. et al. Responses of canopy duration to temperature changes in four temperate tree species: relative contributions of spring and autumn leaf phenology. *Oecologia* 161, 187–198 (2009). <https://doi.org/10.1007/s00442-009-1363-4>

Vitasse, Y., Baumgarten, F., Zohner, C.M., Kaewthongrach, R., Fu, Y.H., Walde, M.G. and Moser, B. (2021), Impact of microclimatic conditions and resource availability on spring and autumn phenology of temperate tree seedlings. *New Phytol*, 232: 537–550. <https://doi.org/10.1111/nph.17606>

Vogt, Gillner, S., Hofmann, M., Tharang, A., Dettmann, S., Gerstenberg, T., Schmidt, C., Gebauer, H., Van de Riet, K., Berger, U., & Roloff, A. (2017). Citree: A database supporting tree selection for urban areas in temperate climate. *Landscape and Urban Planning*, 157, 14–25. <https://doi.org/10.1016/j.landurbplan.2016.06.005>

Vogt, J. M., & Fischer, B. C. (2014). A Protocol for Citizen Science Monitoring of Recently-Planted Urban Trees. In *Cities and the Environment (CATE)* (Vol. 7, Issue 2).

Wallace, C., Walker, J., Skirvin, S., Patrick-Birdwell, C., Weltzin, J., & Raichle, H. (2016). Mapping Presence and Predicting Phenological Status of Invasive Buffelgrass in Southern Arizona Using MODIS, Climate and Citizen Science Observation Data. *Remote Sensing*, 8(7), 524. MDPI AG. Retrieved from <http://dx.doi.org/10.3390/rs8070524>

Walther, G. R., E. Post, P. Convey, A. Menzel, C. Parmesan, T. J. C. Beebee, J. M. Fromentin, O. Hoegh-Guldberg, and F. Bairlein. 2002. Ecological responses to recent climate change. *Nature* 416: 389– 395.

Wang, T., Ottlé, C., Peng, S., Janssens, I. A., Lin, X., Poulter, B., Yue, C., & Ciais, P. (2014). The influence of local spring temperature variance on temperature sensitivity of spring phenology. *Global Change Biology*, 20(5), 1473–1480. <https://doi.org/10.1111/gcb.12509>

White, M. A., Nemani, R. R., Thornton, P. E., & Running, S. W. (2002). Satellite evidence of phenological differences between urbanized and rural areas of the eastern United States deciduous broadleaf forest. *Ecosystems*, 5(3), 260–273. <https://doi.org/10.1007/s10021-001-0070-8>

Williams, C. J., Snyder, K. A., & Pierson, F. B. (2018). Spatial and temporal variability of the impacts of pinyon and juniper reduction on hydrologic and erosion processes across climatic gradients in the western US: A regional synthesis. *Water*, 10(11), 1607. <https://doi.org/10.3390/w10111607>

World Bank. Urban Development. (2020, April 20). Retrieved July 12, 2022, from <https://www.worldbank.org/en/topic/urbandevelopment/overview#1>

Wright, S. J., and O. Calderón. 2018. Solar irradiance as the proximate cue for flowering in a tropical moist forest. *Biotropica* 50: 374– 383.

Xie, Y.; Wang, X.; Silander, J.A., Jr. Deciduous forest responses to temperature, precipitation, and drought imply complex climate change impacts. *Proc. Natl. Acad. Sci. USA* 2015, 112, 13585–13590.

Zhang, X., Friedl, M. A., Schaaf, C. B., Strahler, A. H., & Schneider, A. (2004). The footprint of urban climates on vegetation phenology. *Geophysical Research Letters*, 31(12). <https://doi.org/10.1029/2004GL020137>

Zhang, X., Jayavelu, S., Liu, L., Friedl, M. A., Henebry, G. M., Liu, Y., Schaaf, C. B., Richardson, A. D., & Gray, J. (2018). Evaluation of land surface phenology from VIIRS data using time series of PhenoCam imagery. *Agricultural and Forest Meteorology*, 256–257, 137–149. <https://doi.org/10.1016/j.agrformet.2018.03.003>

Zhang Yehua, Yin Peiyi, Li Xuecao, Niu Quandi, Wang Yixuan, Cao Wenting, Huang Jianxi, Chen Han, Yao Xiaochuang, Yu Le, Li Baoguo, The divergent response of vegetation phenology to urbanization: A case study of Beijing city, China, *Science of The Total Environment*, Volume 803, 2022, 150079, ISSN 0048-9697, <https://doi.org/10.1016/j.scitotenv.2021.150079>.

Zhou, Zhao, S., Zhang, L., & Liu, S. (2016). Remotely sensed assessment of urbanization effects on vegetation phenology in China's 32 major cities. *Remote Sensing of Environment*, 176, 272–281. <https://doi.org/10.1016/j.rse.2016.02.010>

Zipper, S. C., Schatz, J., Singh, A., Kucharik, C. J., Townsend, P. A., & Loheide, S. P. (2016). Urban heat island impacts on plant phenology: Intra-urban variability and response to land cover. *Environmental Research Letters*, 11(5). <https://doi.org/10.1088/1748-9326/11/5/054023>